CHEMICAL REVIEWS

REVIEW

pubs.acs.org/CR

Noncarbon Support Materials for Polymer Electrolyte Membrane Fuel Cell Electrocatalysts

Yan-Jie Wang,[†,‡] David P. Wilkinson,[*,†,‡] and Jiujun Zhang[*,‡]

[†]Department of Chemical and Biological Engineering, University of British Columbia, Vancouver, British Columbia V6T 1Z4, Canada

[‡]Institute for Fuel Cell Innovation, National Research Council Canada, Vancouver, British Columbia V6T 1W5, Canada

CONTENTS

1. INTRODUCTION

In recent years, fuel cells, in particular the proton exchange membrane (PEM) fuel cells, have been demonstrated to be feasible energy converters that convert chemical energy of fuels such as hydrogen directly to electrical energy with high power density, high efficiency, and low to zero emissions. Their applications have been identified in the power demanding areas such as portable, transportation, as well as stationary. This fuel cell technology has also been shown to be competitive with conventional energy conversion devices such as internal combustion engines and batteries, and therefore is expected to be an important energy technology for the future.[1−8] However, there are still several challenges that hinder fuel cell commercialization, including insufficient durability/reliability and high cost. With respect to both of these challenges, PEM fuel cell catalysts have been identified to be the major contributors.

In terms of low durability of PEM fuel cell catalysts, the corrosion of carbon support materials has been identified to be the major contributor to the catalyst failure, in particular for platinum (Pt)-based catalysts, although other failure modes have also some contribution to the catalyst degradation such as Pt dissolution, sintering, as well as agglomeration. With the current state of technology, the state-of-the-art and the most practical electrocatalysts for PEM fuel cells are still carbon-supported Pt catalysts.[9] Unfortunately, carbon supports for these practical Pt-based catalysts are not stable enough for fuel cell durability. For example, during fuel cell operation, in particular for conditions of dynamic load operation in automotive applications, the cathode catalyst will experience high electrode potential in the presence of oxygen at low to zero load during load cycling.[10] Oxidation of the carbon support to produce CO_2 can occur, resulting in the separation of Pt particles from the carbon support and loss of performance. These separated Pt particles would become electronically isolated, leading to a low Pt utilization as well as degraded fuel cell performance. For the anode catalyst, the carbon support can also be oxidized in the situation of fuel (hydrogen) starvation.[11−13] With respect to the instability of carbon materials in fuel cell environments, as stated by Mathias et al.,[10] the carbon materials (Vulcan XC-72R and Ketjen) currently used with fuel cell catalysts do not meet the durability requirements for automotive applications. Therefore, it is necessary to explore stable alternatives

Received: February 20, 2010
Published: September 16, 2011

to replace carbon materials for the catalyst support to improve the durability of PEM fuel cells.

Regarding catalyst supporting strategy, it is commonly recognized that the catalyst support plays a critical role in both catalyst activity and durability.[14−16] To achieve a high performing fuel cell catalyst, the catalyst support should have several important properties including excellent electronic conductivity, high corrosion resistivity, uniform particle size distribution, high surface area, strong cohesive force to catalyst particles, easy formation of uniform dispersion of catalyst particles on their surface, etc. For example, the most used catalysts currently in PEM fuel cells are Pt or Pt alloy-based catalysts supported on carbon materials, which are porous conductive materials with a high specific surface area of >100 m^2/g.[17] Unfortunately, although these carbon supports are outstanding in some respects in terms of their large surface area, high electrical conductivity, and pore structures,[18−21] the corrosion caused by electrochemical oxidation in a PEM fuel cell operating environment has been identified to be the major drawback in terms of catalyst durability and reliability.

Currently, higher temperature PEM fuel cells are considered to be the next generation of PEM fuel cell technology because they have several advantages over cells operated at <90 °C.[22−24] These advantages can be summarized as: (1) improved fuel cell reaction kinetics, especially for the cathode oxygen reduction reaction (ORR); (2) small increased catalyst tolerance toward contamination; (3) improved heat rejection capability; and (4) improved water management. Unfortunately, when PEM fuel cells are operated at higher temperatures (90−200 °C), catalyst support corrosion is even more severe, leading to a higher degradation of the performance. For example, during long-term fuel cell operation (>500 h) at higher temperatures, the oxidation of the carbon support has clearly been observed in our work.[25,26] This was typically accompanied by a loss in electro-catalytic surface area, suggesting that the Pt particles were either separated from the carbon supports due to the oxidation of the carbon or agglomerated into larger sizes. The situation became even worse when the fuel cell was operated at an extremely high temperature (300 °C). It was observed that the fuel cell performance was degraded within hours of operation, and MEA diagnosis showed significant corrosion of the carbon support.[27] Therefore, development of more durable catalysts and catalyst supports for PEM fuel cells is required for higher temperature PEM fuel cell operation, that is, >90 °C.

To address the issue of catalyst support corrosion, some alternative support materials rather than the traditional carbon-based supporting materials in PEMFCs,[22−24] should be explored. For these noncarbon materials for fuel cell catalyst supports, some basic requirements should be met, including high surface area, favored dispersion of catalytic metals, high corrosion resistance under both dry and humid air conditions and at both low and high temperature, low solubility in acidic or alkaline media, high electrochemical stability under fuel cell operating conditions, as well as high conductivity. In addition, the noncarbon supporting materials should have a strong physicochemical and electronic interaction with catalytic metals to improve their catalytic activity and durability.[28,29] With respect to the exploration of noncarbon support materials for fuel cell catalysts, considerable work has been done in the past decades. The materials developed include metal,[15,30−33] nitride,[34] carbide,[34,35] mesoporous silicas,[36,37] conducting polymers,[38,39] as well as metal oxides.[40] In this Article, the developments for several important kinds of noncarbon supporting materials in recent years are reviewed. The challenges for developing noncarbon supporting materials are analyzed, and the possible future research directions, in particular the material preparation methods, are also proposed in this Article.

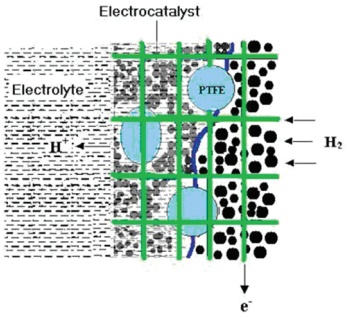

Figure 1. Components in the structure of a gas diffusion fuel cell electrode. Reprinted with permission from ref 43. Copyright 2004 Royal Society of Chemistry.

2. IMPACT OF CATALYST SUPPORT IN PEM FUEL CELLS

2.1. Relationship between Support and Electrode

Since Bacon[41] found an appreciable current density using a dual-porosity structured electrode in 1960, a lot of scientists have attempted various electrodes to further improve the performance of fuel cells. Each significant advance in materials development has led to a new generation of fuel cells. Figure 1 shows the structure and components of an electrode used in conventional low temperature PEM fuel cells. These components of an electrode are polytetrafluoroethylene (PTFE), high surface area catalyst support (for example, carbon) loaded with precious metal catalysts, a current collector, and possibly other minor components.[42] Typically, the electrochemical reaction in hydrogen−oxygen fuel cells, which occurs at the anode, is

$$H_2 \rightarrow 2H^+ + 2e \quad (1)$$

and the complementary reaction occurring at the cathode is

$$O_2 + 4H^+ + 4e \rightarrow 2H_2O \quad (2)$$

In Figure 1, the sequential processes involved for the gas diffusion fuel cell anode are the dissolution of hydrogen gas at the gas−electrolyte interface, diffusion of dissolved hydrogen to the electrolyte−catalyst interface, electrochemical reaction at the catalyst−electrolyte interface, conduction of electrons by the current collector, and proton transport across the electrolyte (for PEM fuel cells, the electrolyte is a proton exchange membrane such as Nafion). Chanetal et al.[43] have pointed out that there are a number of factors that play a role in determining the best electrode materials and structure to use. Such factors include the chemical compositions and morphologies of components, high surface area for maximum reaction rate and high porosity for fast mass-transport, optimization of the solid phase and the continuous liquid phase for best electronic and ionic transport, wettability, gas−liquid interphase mass transport, and the stability, length, and thickness of the three-phase boundry, etc. Perhaps the most important issue for electrode performance would be the choice of electrocatalyst for a given charge transfer reaction. In particular, the support for the metal electrocatalyst turns out to be as important as the nanoparticles for providing their

dispersion performance and stability. In addition to electrical conductivity and surface area, hydrophobicity, morphology, porosity, and corrosion resistance are also important factors in the choice of a good catalyst support. Because the platinum precursor can be uniformly dispersed on its surface by the hydrophilic morphology and porosity of support, Yu and Ye[44] have obtained the optimized Pt particle size, dispersion, and adhesion properties for a good catalyst.

2.2. Effect of Support on Catalytic Stability and Activity

Currently, PEM fuel cells are operated at low temperatures usually less than 80 °C. At low temperatures, several issues have been identified: PEM fuel cell reaction kinetics, in particular the slow ORR, can hinder improvements in fuel cell performance and require larger Pt catalyst loadings; the tolerance of the catalyst toward contamination is insufficient; heat rejection is slow; and water management in the system is difficult. Therefore, to overcome these obstacles, it is desirable to operate at higher temperatures above 80 °C. ORR kinetics becomes significantly more rapid at high temperatures, while the water flooding issues are reduced.[45,46] However, the degradation of the catalyst and the support will also be accelerated. During long-term PEM fuel cell operation, the oxidation of the carbon support and growth of the Pt catalyst particles with a corresponding decrease in electrocatalytic surface area is clearly observed.[47] Long-term operation can also change the MEA properties from hydrophobic to hydrophilic resulting in electrode flooding, which will significantly decrease performance. Figure 2 showed the possible degradation mechanisms.[25,48] The proposed mechanism of Pt particle growth in Figure 2a showed that platinum ions transport through the liquid and/or ionomer while electrons transport through the carbon support. Free electron concentration in carbon is quite high. Thus, transport of electrons through carbon support is rapid and is not rate limiting. That is, when in contact with carbon, the particles will essentially be at the same electrostatic potential. The overall reaction may then be given by a dissolution and a precipitation as follows:

(1) Pt^0 (smaller particle) → Pt^{2+} (liquid and/or ionomer) + 2e (carbon).

(2) Pt^{2+} (liquid and/or ionomer) + 2e (carbon) → Pt^0 (larger particle).

It is clear from Figure 2b that in most typical anodes, Pt (or Pt and Ru) supported on carbon particles is prone to degradation during fuel starvation due to reaction 3, the oxidation of carbon, which is catalyzed by the presence of platinum.[49] This reaction proceeds at an appreciable rate at the electrode potentials required to electrolyze water in the presence of platinum (greater than approximately 1.4 V[50]).

$$C + 2H_2O \rightarrow CO_2 + 4H^+ + 4e^- \quad (3)$$

The carbon catalyst support is converted to CO_2, and Pt and/or Ru particles may be lost from the electrode, resulting in loss of performance.

Besides carbon oxidation, catalyst sintering or agglomeration is another problem for the reduction of a PEM fuel cell's durability[51] when operated at higher temperatures. The catalyst sintering could reduce the electro-active surface area of the Pt catalyst, lower the Pt utilization, and degrade its catalytic activity. In particular, carbon support oxidation is only one of the factors that leads to catalyst agglomeration. To avoid this problem, the usage of a noncarbon support such as metal oxides[52−54] or other materials has proved to be very important and significant to obtain good PEM fuel cell performance.

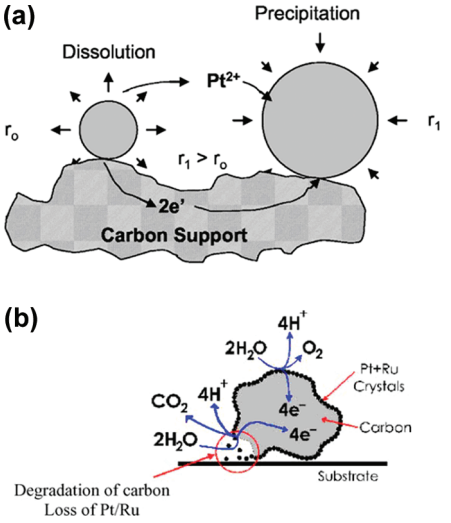

Figure 2. Schematic representations of Pt agglomeration and carbon corrosion. (a) Reprinted with permission from ref 48. Copyright 2007 Electrochemical Chemical Society. (b) Reprinted with permission from ref 25. Copyright 2004 Elsevier B.V.

The use of noncarbon supports can not only reduce the amount of noble metal like Pt but also enhance catalytic activity and stability. To further improve catalytic activity, developing promising noncarbon catalyst supports is necessary in the design and synthesis of new electrocatalysts. In recent years, a lot of researchers have devoted themselves to the fundamental understanding of the ORR mechanism catalyzed by novel material-supported Pt electrocatalysts because the dominant polarization in a PEM fuel cell comes from the slow cathodic oxygen reduction reaction (ORR) rather than the anodic hydrogen oxidation reaction (HOR). Recently, Filhol et al.[55] used first-principle analysis and pointed out that on a fully hydrated Pt{111} surface, electron transfer could precede protonation of the absorbed O_2 molecule. Through a pattern of hydrogen bonding, the proton would bond to the adsorbed O_2 molecule in the form of H_3O^+. Their results were also applied to explain the initial stages of O_2 adsorption and activation as a function of applied potential on well-defined pure Pt and metal-supported Pt and were validated by experimental results.[56] In 2008, Norskov et al.[57] reviewed how the catalytic activity could be affected by the electronic structure and geometric distribution of the nanocomponents in the catalyst. On the basis of Norskov's theoretical research on ORR catalysts, Stamenkovic et al.[58] found that metal-supported Pt electrocatalysts involving 3d metals were better than pure Pt catalyst because the electronic structure on the surface of metal-supported Pt could be slightly modified. This provided useful information for developing and understanding the factors controlling the ORR kinetics with the use of non-carbon-supported Pt catalysts.

2.3. Interaction of Pt with Support

In a supported Pt catalyst system, the physicochemical and electronic interaction between Pt and the support plays an important role in both the catalytic activity and the stability. In general, in the supported Pt PEM fuel cell catalysts, the interaction between the Pt particle with its support can be

attributed to the presence of electronic effects. For the catalytic ORR, the metal−support interaction is through electron transfer from platinum clusters to oxygen atoms adsorbed on the support surface.[59,60] In many cases, chemical bonds can be formed with the charge transfer taking place between the contacting phases.

Electronic interaction between the Pt catalyst particle and the support has been investigated by conventional physical, spectroscopic, and electrochemical studies. For example, electron-spin resonance (ESR) studies have demonstrated the electron donation by platinum to the carbon support.[61] This has been further supported by X-ray photoelectron spectroscopy (XPS) studies[62] showing that the metal can act as an electron donor to the support, and the interaction is dependent on the Fermi level of electrons in both. In the XPS studies, the Pt 4f7/2 signal for the carbon-supported pure Pt catalyst was found to be shifted to higher binding energies with respect to that of unsupported platinum due to the platinum-support electronic effect.[63,64] For carbon-supported PtRu catalyst, Antolini et al.[65] revealed a further shift to high energy values for the Pt 4f7/2 signal of PtRu/C by 0.2−0.3 eV with respect to a pure Pt/C catalyst. This further shift for PtRu/C was attributed to the strong platinum−support interactions or small particle effect. Furthermore, the presence of Ru precursors and their decomposition could also affect the acid−base properties of the carbon support. This effect should produce a strong metal−support interaction, which then affects the electronic nature of the platinum sites. Goodenough and Manoharan[66] combined the observation from XPS, extended X-ray absorption fine structure (EXAFS), and ESR measurements on a carbon-supported PtRu catalyst and concluded that the synergistic catalytic effect could result from an intra-alloy electron transfer from Ru to Pt. McBreen and Mukerjee[67] studied the Pt X-ray absorption near-edge structure (XANES) at 0.0, 0.24, and 0.54 V at the respective Pt L3 and L2 edge using both Pt/C and PtRu/C catalysts and observed that alloying with Ru could cause electronic effects on the Pt. Kim et al.[68] studied a pure Pt−Ru bimetallic alloy and analyzed the surface chemical composition and oxidation state of each metal by Pt 4f and Ru 3p XPS spectra, and they observed the electron transfer between Pt and Ru. Lim et al.[14] instigated a TiO_2 nanotube-supported Pt catalyst by XPS. Although the Ti peak was not detected due to the Pt coating layer (~20 nm outside of the TiO_2 nanotube), the binding energy of Pt 4f7/2 in the XPS profiles for the Pt/TiO_2 nanotube catalyst was found to slightly shift in the positive direction, which was thought to be the Pt−TiO_2 nanotube interaction. This Pt−support interaction was considered to be beneficial to the enhancement of both the catalytic activity and the stability improvement of the electrocatalyst.[69,70] According to Bogotski and Snudkin,[71] the change in electrocatalytic activity was attributed to the electronic state of Pt when deposited on a carbon support. In their explanation, an electrical double layer can be formed on the support where the microdeposited (Pt) particle is located, thereby resulting in an increase in electron density on the platinum. This rise in electron density can be significant only if the particle size of the microdeposit (Pt) is comparable to the thickness of the double layer.[72] Therefore, the particle size of the catalyst metal crystallite does influence the catalyst support interaction and/or synergism.

Additionally, it was reported[73,74] that during supported Pt catalyst formation, the interaction of the Pt precursor with the support is crucial and can affect the Pt particle size and dispersion, as well as adhesion properties. For a carbon-supported Pt catalyst system, the reduction of H_2PtCl_6 precuser into a Pt(II) complex on the carbon particle surface plays an important role in forming active catalysts.[73−75] On the other hand, the carbon surface basic sites can act as anchoring sites for the hexachloroplatinic anion, which is considered responsible for the strong adsorption of platinum on carbon. The carbon surface basic sites are frequently associated with pyrone-like structures, which would have a strong electronic interaction with the surface carboxyl groups. According to other researchers,[76−78] the surface basic sites are essentially of the Lewis type and are associated with π-electron rich regions within the basal planes. Leon et al.[78] thought that the protonation of such oxygen-free basic carbon sites would lead to an electron−donor−acceptor complex. Lambert and Che[79] provided an alternative formulation of the model for the strong adsorption of $PtCl_6^{2-}$ using the mechanism of inner-sphere adsorption. In their model, surface groups would replace some of the original ligands (Cl^-) of the transition metal in solution.

3. METALS AS CATALYST SUPPORTS

To reduce the usage of expensive Pt and at the same time to improve the catalyst activity toward fuel cell reactions, one of the approaches is to develop some cost-effective metal-supported Pt catalysts. A typical metal-supported catalyst contains metal support particles and the metal catalyst particles. In the art, the metal support particles provide a physical surface for dispersion of smaller catalyst particles to achieve a high surface area. In some synthesis cases, the formed catalysts might be sintered at high temperatures to increase the attachment between the support and the catalyst particles. This process can produce some degree of alloying between the catalyst metal and the metal support, leading to improved catalyst activity and durability. The strong physicochemical and electronic interaction between the metal support and the catalyst particles can generate a bifunctional mechanism for catalytic reaction, benefiting the reaction kinetics. For example, when Pt and Ru form alloying catalysts, the catalytic activity of the alloy catalyst toward methanol or CO oxidation becomes much faster. With respect to this, a great amount of research on Pt−Ru alloys has been reported in the literature since the 1960s,[80−82] in which ruthenium has been identified to be the best promoter for Pt catalytic activity toward the electrooxidation of methanol. For Pt-based catalysts in PEM fuel cell reactions,[83−87] several metals have been explored for metal supports, including Ru, Pd, Ag, Ir, Rh, Au, Re, Os, as well as Co.

Frelink et al.[88] deposited Ru on Pt (111) electrode and examined the framework of a bifunctional mechanism for CO adsorption and electrooxidation by IR spectroscopy. It was found that adsorbed CO on Pt−Ru could be oxidized at a potential more negative than that on pure Ru, leading to higher activity for CO electrooxidation. An electrochemical quartz crystal microbalance (EQCMB) technique was also employed to probe the bifunctional mechanism of CO electrooxidation catalyzed by Ru−Pt catalyst.[89] In addition, the Ru surface coverage on the Pt was also optimized with respect to the catalytic activity. It was found that the optimum amount of Ru surface coverage for both CO and CH_3OH electrooxidation was about 15%. Later, Chrzanowski and Wieckowski[90] prepared some ultrathin Ru ultrathin films on platinum single crystal surfaces, Pt(100), Pt(111), and Pt(110), respectively, using a spontaneous deposition method. Electrochemical measurements indicated that all such Ru films were stable in the electrode potential range before the platinum

oxidation potential. An alternative approach was to deposit Pt on Ru. The electrocatalysts made by this approach could not only reduce the Pt usage as compared to that of pure Pt catalysts but also improve catalytic activity. Brankovic et al.[91,92] reported a Pt−Ru bimetallic electrocatalyst, in which Pt was deposited on a Ru(0001) single crystal surface. A strong interaction between Pt and Ru was found and attributed to the electronic modification of the Pt adlayer by the Ru substrate. The electrochemical behavior of Pt/Ru bimetallic surfaces shows a distinct dependency on the thickness and morphology of the Pt deposits, which could be of interest for the design of Pt/Ru catalysts. The electrocatalytic properties of this supported Pt/Ru catalyst showed some enhanced CO tolerance at a considerably lower Pt loading than that of commercially available Pt/Ru catalysts.

Besides Ru, Sasaki et al.[93] prepared a Au(111)-supported Pt electrocatalyst, in which a Pt submonolayer was deposited on Au nanoparticles. The voltammetry curve obtained on this surface indicated the presence of both Pt and Au on the surface. Zhang et al.[94] synthesized some catalysts, in which Pt monolayers were deposited on a Pd(111) surface to form ORR catalysts. The ORR kinetics was studied using a rotating disk-ring electrode technique in acidic solution. The experimental results showed a significant enhancement in the ORR catalyzed by the Pt monolayer on the Pd(111) surface when compared to that catalyzed by Pt(111). The noble metal mass-specific activity of this Pt−Pd catalyst also was 2 times higher than that of Pt/C catalyst.

On the basis of an investigation of Pt morphology and structure on metal supports, Stamenkovic et al.[95] found that the ORR kinetics were strongly dependent on the arrangement of Pt on the surface region of metal support. For example, bulk Ni-supported Pt (PtNi) and Co-supported Pt (PtCo) alloy surfaces have a Pt-skeleton surface and Pt-skin surface, respectively. Here, due to the thermodynamics of surface segregation, annealed alloy surfaces could form the outermost Pt surface layer, which then served as the Pt-skin surface.[95,96] The Pt-skin surface formed in ultrahigh vacuum (UHV) were found for all three Pt_3M alloys (M = Co, Ni, Fe, etc.), which were very stable in terms of physicochemical properties when they were immersed in an acidic solution. Other Pt surface, called Pt-skeleton surface, could also be formed when a Pt−M alloy (M is a transition metal) was exposed to the acidic environment. In this acidic environment, transition metal atoms in the surface layer could be dissolved, resulting in an outermost layer, only containing Pt.[97,98]

Stamenkovic et al.[95] believed that the arrangement of Pt on the surface of a metal support becomes very important for catalytic activity, and that the catalytic activity at different surfaces was in the order of Pt_{bulk} < Pt-skeleton < Pt-skin-monlayers. Their results showed that, as compared to Pt(111) catalyst, a 10-fold improvement in the oxygen reduction reaction (ORR) activity was obtained using bulk Ni(111)-supported Pt catalyst. This catalyst gave a 90-fold greater activity than current state-of-the art Pt/C catalysts for PEM fuel cells. The bulk Ni(111)-supported Pt catalyst like Pt_3Ni has been studied as the most active cathode catalyst.[99]

Zhang et al.[100] also deposited a Pt monolayer on either a Au(111), Rh(111), Pd(111), Ru(0001), or Ir(111) surface to form ORR catalysts. The ORR activity of these catalysts showed a volcano-type dependency on the d-band center of the platinum monolayer structures. Their results showed that for a better ORR electrocatalyst, both the breaking of the adsorbed O−O bond on the catalyst surface and the hydrogenation of the corresponding reactive intermediates have to be facile. Theoretical studies on

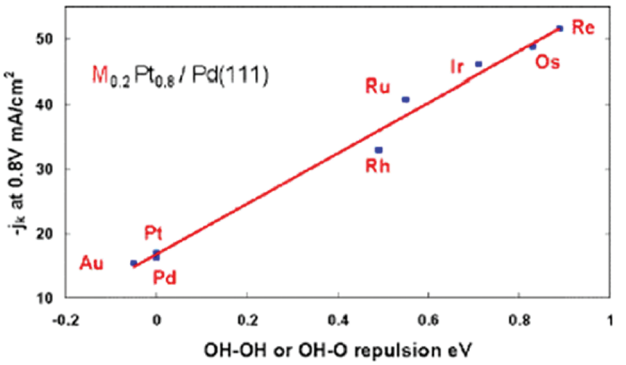

Figure 3. Relationship between kinetic current at 0.80 V and the repulsive 60 interaction in seven different $(Pt_3M)ML/Pd(111)$ (2×2) unit cells, as compared to PtML/Pd(111), characterized by the calculated interaction energy between two OHs, or OH and O. Reprinted with permission from ref 101. Copyright 1990 American Chemical Society.

the ORR mechanism catalyzed by a metal-supported PtM layer indicated that the removal of adsorbed OH from the Pt surface could be the rate-determining step in the overall ORR process.[101] They also showed that for PtM with M = Rh, Ir, Ru, Os, or Re, OH coverage on Pt can be reduced effectively, leading to faster ORR kinetics. Figure 3 shows the kinetic currents as a function of effective repulsion energy between two OHs, or between the O and OH, on a mixed PtM monolayer (M = Au, Pd, Rh, Ru, Ir, Re, or Os) deposited on a Pd(111) surface. A linear correlation in this figure indicates that the reduced OH overage on Pt can be attributed to a lateral repulsion between the adsorbed OH on Pt and the adsorbed OH or O on the neighboring M metal atom. As a result, the kinetic current density for the ORR on this mixed PtM monolayer becomes more than 3 times larger than that on a pure Pt monolayer. This is in agreement with the fact that the ORR activity of such a Pt monolayer is more active than that of pure Pt(111). The oxidation of Pt in this mixed PtM monolayer could be highly suppressed, only occurring at a significantly higher potential greater than 1.17 V (vs SHE).

In addition to Pt, other transition metals such as Pd, Ag, Ir, Ru, Rh, Au, Re, and Os have also been explored as a deposited monolayer on the surfaces of other metal to increase catalytic activity and at the same time to reduce noble metal loadings. Naohara et al.[102] synthesized Pd thin-layer coated Au particles and tested them for ORR activity. The catalysts formed exhibited a strong ORR activity. Brankovic et al.[103] deposited Pd on a Ru(001) single crystal surface with the amount of deposited Pd indirectly controlled by the Pd ion concentration in the solution. The initial Pd growth involved formation of an ordered monolayer, while further growth resulted in the formation of a three-dimensional Pd deposit. Using a Cu adlayer as a template, this group[104] also prepared three other electrocatalysts, Pt−Au, Pd−Au, and Ag−Au, respectively. The formed Pt submonolayer was two-dimensional with partially interconnected nanoclusters of monatomic height. However, Pd formed a uniform, but textured monolayer, while Ag formed a bilayer. The deposition layer of each metal uniformly covered the entire gold surface without preferential deposition along the step edges. Additionally, they also deposited other transition metal such as Ir, Ru, Rh, Pd, Au, Re, or Os as a monolayer on the surfaces of Pd(111) single crystals. High ORR activity of these catalysts was achieved, demonstrating a new way of synthesizing ORR catalysts through

the modification and control of the surface reactivity of catalyst metal monolayers.

4. NITRIDES

Recently, transition metal nitrides, some of which also possess catalytic activity that are similar to those of noble metals like Pd and Pt, have been reported as catalyst supports.[105−107] However, in terms of fuel cell applications, so far, there are not many publications dealing with metal nitrides as catalyst supports. Among different metal nitrides, titanium nitride (TiN) seems to be the most widely studied.[108] The nanostructured TiN has proven to be a promising material for super capacitors,[109] and its application as an electrode material has also been reported in the literature.[109−115] Because of its higher electrical conductivity and outstanding oxidation and acid corrosion resistances,[116−118] TiN should be a useful catalyst support for PEM fuel cells, especially for high temperature PEM fuel cells, to replace carbon materials. In the literature,[114] Musthafa and Sampath reported that electrodeposited Pt on TiN film coated on a stainless steel substrate showed a higher activity than the conventional electrocatalyst for methanol electrooxidation. According to Datta and Kumta,[110] the Pt/Ru alloy supported on TiN as an anode catalyst shows a high catalytic activity in direct methanol fuel cells (DMFCs). Recently, Avasarala et al.[118] reported TiN nanoparticles as a catalyst support for Pt-based catalysts for the PEM fuel cell anode. Transmission electron microscopy (TEM) analysis for the Pt/TiN electrocatalyst showed that the average particle size was ∼2 nm, as shown in Figure 4, with a distribution range of 1−3 nm, and the X-ray mapping suggested an uniform distribution of Pt on the TiN support. In electrochemical measurements, this Pt/TiN catalyst exhibited a higher catalytic ORR activity than that of commercially available 20 wt % BASF Pt/C catalyst. Unfortunately, in terms of long-term stability, the chemical stability of TiN in acidic solution appears to be too poor to be used as a catalyst support for PEM fuel cells where the reaction medium is acidic. According to Avasarala et al.,[119] some factors such as concentration and type of acid media can strongly influence the TiN surface. Passivation behavior was observed for TiN due to surface hydrolysis, which could be affected by both the temperature and the concentration of the acid electrolyte, for example, perchloric acid.

Boron nitride (BN) is another potential candidate for a catalyst support. This chemical with a hexagonal structure, as shown in Figure 5, is similar to that of graphite.[120,121] Its thermal properties, such as thermal stability, thermal conduction, and thermal transport, and chemical inertness with respect to less dissolution and chemical reactivity are promising for applications under harsh conditions. Recent research[122,123] showed that finely ground BN powder, which had high thermal conductivity within a range of 4−6.2 W/cm·°C,[124] thermal stability under 1000 °C, high acid−base and oxidation resistances (the conditions for oxidation resistance should be determined by the chemical reactivity between BN and air/other oxide compound material), and appropriate mechanical resistance, suggesting enough strength and stable mechanical property to be used as a supporting material for electrocatalysts, could be used as a support for Pt catalysts. To increase the high surface area of BN powder, Perdigon-Melon et al.[125] prepared porous BN samples using different chemical precursors. They found that porous BN obtained by the sol−gel deposition method was a better support for a highly dispersed Pt catalyst than BN powder directly

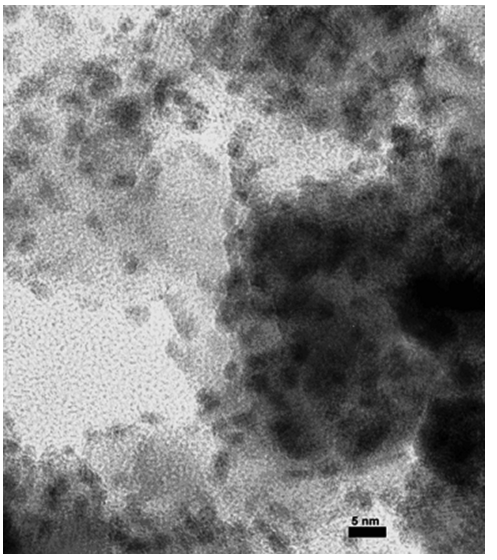

Figure 4. TEM image of Pt/TiN particles. Dark spots are Pt particles (scale bar: 5 nm). Reprinted with permission from ref 118. Copyright 2009 Royal Society of Chemistry.

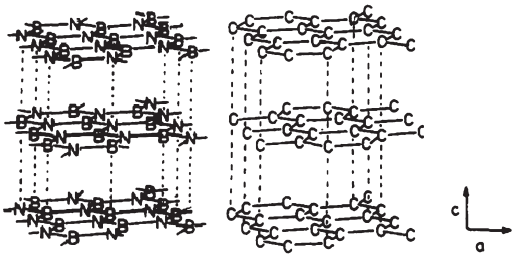

Figure 5. Comparison of graphite structures for both BN and C. The lattice spacing, $c/2$, is 3.33 Å for BN and 3.35 Å for C. Reprinted with permission from ref 121. Copyright 1990 American Chemical Society.

synthesized from a precursor mixture. More platinum could be scattered on the surface of the support powder, which was confirmed by both elemental analysis and XPS measurements, as shown in Table 1.

In addition, molybdenum nitride (Mo_2N) and molybdenum carbides (Mo_2C) were reported to be active for the water gas shift (WGS) and methanol steam reforming (MSR) reactions.[126−130] These materials also possess some catalytic properties that are similar to those of noble metals like Pd and Pt.[105−107] For example, Setthapun et al.[34] synthesized some promising MSR catalysts using a parallel synthesis system, in which some metals including Co, Cu, Fe, Ni, Pd, Pt, Ru, and Sn were supported onto a high surface area Mo_2N or Mo_2C support.

5. CARBIDES

Carbides are compounds composed of carbon and a less electronegative element. According to chemical bonding types, all carbides exhibit some level of covalent character. They can be classified into four categories as follows: (1) salt-like, (2) covalent compounds, (3) interstitial compounds, and (4) "intermediate" transition-metal carbides (TMCs).[131] Among these categories, TMCs, which are stable in acidic and basic solutions, of low cost, and are CO tolerant in the temperature range of

Table 1. Results from Characterization of the BN-Supported Pt Catalyst Samples[a]

				XPS measurements (wt %)		
sample	surface ($m^2\ g^{-1}$)	L_c (nm)	classical measure (wt %)	B	N	Pt
A	110	3.7	4.1	44.4	47.2	0
B	500	1.6	1.6	37.4	44.3	1.5

[a] A: A direct synthesis of platinum supported on BN powder starting from a precursor mixture. B: A two-step preparation from a BN powder obtained from P I followed by an impregnation using a sol−gel method. Reprinted with permission from ref 125. Copyright 2004 Elsevier B.V.

353−373 K,[132] are identified as promising substitutes for noble metal catalysts due to their similar, and in some cases better catalytic activity as compared to noble metals.[105,132,133] In the following, carbides used as supports for noble metal catalysts are reviewed.

5.1. Boron Carbide (B_4C)

Boron carbide (B_4C), which is considered a "covalent carbide", is a hard material and refractory. In 1963, boron carbide was first mentioned as an electrode material due to its good conductivity, corrosion resistance, and oxidative stability.[108] During 1965−1966, Grubb and McKee[134,135] showed that boron carbide when used as a catalyst support for platinum could enhance the platinum catalytic activity in phosphoric acid fuel cells. Furthermore, platinum on boron carbide was found to be more resistant to sintering than platinum on graphite at an equal surface coverage. It was also observed that the catalyzed adsorption of hydrogen that normally occurs on graphitic carbon did not occur on boron carbides. In 1969, McKee et al.[136] tested a carbide-supported catalyst (Pt/Ir supported on boron carbide) in ammonia/oxygen alkaline fuel cells. The fuel cells were operated at 100−120 °C using 54% potassium hydroxide as electrolyte. The cell resistance was observed to be higher if the boron carbide-supported Pt/Ir alloy catalyst was used, that is, 0.3−0.35 Ω versus 0.2−0.25 Ω. When used as an anode in a cell, boron carbide-supported Pt/Ir alloy catalyst showed lower open-circuit potentials (0.180 vs 0.255 V) and lower polarization performance than the graphite-supported Pt catalyst. Unfortunately, the anodes catalyzed by boron carbide-supported Pt/Ir catalyst, as compared to those catalyzed by graphite-supported catalyst, were generally less reproducible because of the ammonia−deuterium exchange and the gas-phase decomposition of ammonia. The exchange of ammonia with deuterium took place at a rapid rate over the iridium black at 25 °C.

5.2. Titanium Carbide (TiC)

Titanium carbide was investigated as a useful electrode material in electrolytic cells.[108] It was known that titanium carbide was stable in the electrolytic oxidation of manganese sulfate to MnO_2 at current densities exceeding 100 A/ft^2.[137] Up to now, there is only limited literature reporting titanium carbide-supported catalysts. Jalan et al.[138] showed that titanium carbide with a relatively large average surface area of 25−125 m^2/g could be prepared by putting titanium tetrachloride in a gas flow stream containing unsaturated hydrocarbon and hydrogen in the range of 500−1250 °C. In this process, a titanium carbide was formed with a desirable chain-like structure and favored open porosity as well. The open porosity can maintain electrical contact and provide paths for oxygen diffusion. The Pt surface area was found to be in the range of 20−90 $m^2\ g^{-1}$ for the TiC-supported Pt catalyst. It was expected that this support could improve both the electrochemical corrosion resistance and the catalytic activity in fuel cells.

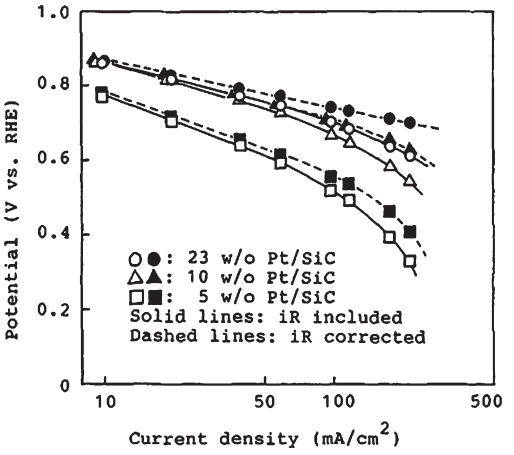

Figure 6. Potential−current density plots for oxygen reduction on electrodes (0.6 mg Pt/cm^2) using platinum supported on silicon carbide electrocatalysts in 98 w/o phosphoric acid at 190 °C. Reprinted with permission from ref 142. Copyright 1988 Electrochemical Chemical Society.

5.3. Silicon Carbide (SiC)

With high-temperature stability up to 1200 °C in an oxidative environment,[139] hardness, as well as chemical inertness, silicon carbide has been proposed to be an interesting possible catalyst support.[140,141] In 1988, Honji et al.[142] prepared SiC-supported Pt catalysts by chemically reducing chloroplatinic acid with methanol in the presence of both silicon carbide powder and a surface active agent. Silicon carbide was thought to be less electronically conducting due to its low conductivity around 10^{-6} S/cm,[143] so to further improve electronic conduction in the fabrication of the electrode, a carbon black was also used to support the Pt/SiC catalyst. The result showed that platinum particles were well dispersed on the SiC surface, and that among the catalysts synthesized, 23 wt % Pt/SiC on the carbon substrate showed the best polarization, 0.7 V vs RHE at 220 mA cm^{-2} (*iR* corrected, see Figure 6). This value is almost the same as that of a carbon-supported platinum catalyst. In addition, Rao et al.[143,144] attempted to prepare a nano-SiC-supported Pt nanoparticle catalyst in which nano-SiC was obtained from coarse SiC in a thermal plasma. Their electrochemical measurements indicated that the ORR activity and the degradation of performance of the Pt/SiC catalyst were similar to that of the commercially available Pt/C (E-TEK) catalyst, as shown in Table 2. However, according to Krawiec and Kaskel,[145] commercially available silicon carbide with a low specific surface area (S_g < 25 $m^2\ g^{-1}$) is not appropriate for a catalyst support. Considerable efforts have been made[146−151] with a hope that high surface area of SiC would become a valuable catalyst support for fuel cells.

5.4. Tungsten Carbides

Tungsten carbide (WC) is an important industrial material and is widely used, for example, as a coating material for cutting tools. Tungsten carbide was suggested to possess promising catalytic activity in sulfuric acid solutions by Bohm[152] and was later

Table 2. Estimated Pt Loadings, Pt Particle Size, Specific Surface Areas, and Oxygen Reduction Activities for As-Synthesized Pt/SiC and Commercially Available Pt/C Catalysts[a]

catalyst	Pt loading[b] (wt %)	Pt particle[c] (nm)	specific surface area of Pt (m^2 g^{-1})	electroactive surface area[d] (m^2 g^{-1})	ORR activity at +0.85 V vs NHE (A g^{-1})
as-synthesized Pt/SiC	18.4	3.5 ± 0.6	76 ± 1.5	78 ± 8	125
commercial Pt/C (E-TEK)	19.7	3.7 ± 0.2	81 ± 10	85 ± 5	141

[a] Reprinted with permission from ref 143. Copyright 2008 NISCAIR. [b] From spectrophotometric measurements. [c] From TEM measurements. [d] From cyclic voltammetry measurements.

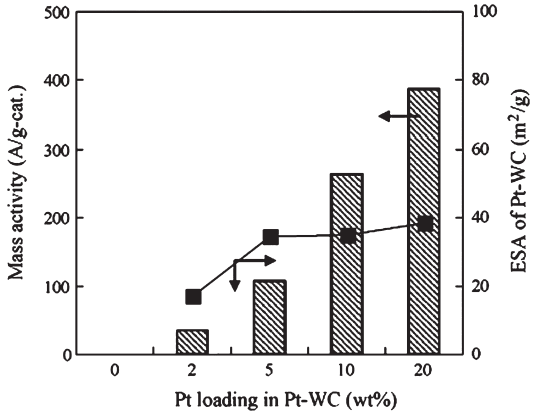

Figure 7. Relationship of electroactivity to Pt loading in the Pt/WC catalyst. Reprinted with permission from ref 176. Copyright 2007 Elsevier B.V.

confirmed by Levy and Boudart.[105] A Pt-like behavior was observed in several catalytic reactions, indicating that tungsten carbide itself could become a promising electrocatalyst or catalyst support due to its unique chemical and physical properties.[153−161] In recent years, a large number of results have been reported on developing tungsten carbide as a support for fuel cell electrocatalysts.

It is well-known that tungsten carbides show some special properties, such as high selectivity with respect to catalytic hydrocarbon reactions,[162] *n*-hexane isomerization,[163] as well as dehydrogenation in hydrazine decomposition,[164] good electrical conductivity (10^5 S/cm for WC at 20 °C),[165,166] and high stability in acid solutions.[167] In general, tungsten carbide exists in different phases, of which the most important are tungsten monocarbide (WC) and tungsten subcarbide (W_2C).[168] As compared to WC, W_2C is thermodynamically unstable at lower temperatures below 900 °C,[165,169,170] WC is produced by traditional metallurgical routes, the obtained WC has a low surface area, which is a major drawback when using it as a catalyst support.

For WC-supported Pt catalysts, tungsten carbides promote catalytic activity through synergistic effects with Pt in fuel cells. In 2003, Liu et al.[171] demonstrated the synergistic effect of WC and Pt on catalytic activity toward the dissociation of methanol, water, and hydrogen. Later, the catalytic activity of WC-supported Pt catalyst toward the dissociation of methanol and hydrogen was also observed by Barnett et al[155] and Zellner et al.[172] Both WC and W_2C were used as supports for Pt catalysts in the methanol electrooxidation reaction and showed high Pt-like activity and insolubility in acid solutions.[173,174] In addition, the Pt/W_2C electrocatalyst also has a strong resistance to catalytic poisons such as carbon monoxide.[157]

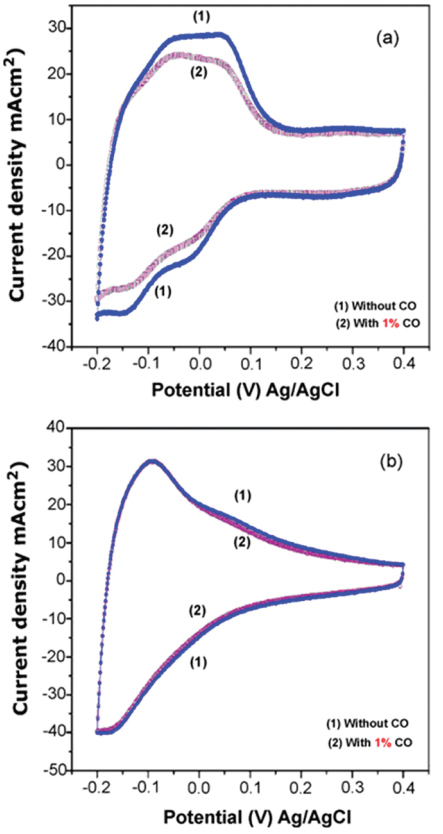

Figure 8. Cyclic voltammogram of (a) commercially available 20 wt % Pt/C (E-Teck) and (b) 7.5 wt % Pt/mesoporous WC in (1) a 1 M H_2SO_4 solution and (2) a 1 M H_2SO_4 solution purging with 1% Co and 99% H_2 gas for an hour under a scan rate of 50 mV/s at 298 K. Reprinted with permission from ref 177. Copyright 2008 Elsevier B.V.

The surface area of WC powder is critical for catalyst activity when used as a support, indicated by Chhina et al.[166] Hara et al.[175,176] synthesized some tungsten carbides by carburizing of W_2N and WS_2 precursors, respectively. Their results indicated that WCs, which were prepared from $W(CO)_6$/S and $(NH_4)_2WS_4$,[175] give a higher surface area (80 m^2/g) than those obtained from the conventional direct carburization of WO_3. Figure 7 illustrates the relationship between the electroactivity (mass activity) and the amount of Pt loading in a Pt−WC catalyst system. It can be seen that the mass activities increase in proportion to the amount of Pt loading. To improve the surface area, Ganesan et al.[174] synthesized two types of mesoporous tungsten carbide as supports for Pt catalysts, which had surface areas of 95 and 76 m^2/g, respectively. These mesoporous tungsten carbide-supported Pt catalysts showed higher activity (2 times higher mass activity) for electrochemical oxidation of

Table 3. Electrocatalytic Activities and CO Tolerances of Pt/WC and Pt/C Catalysts for Hydrogen Electrooxidation[a]

catalyst	condition of electrolyte	electrochemical surface area (m^2/g-Pt)	specific activity at 0.0 V (mA/cm^2)	mass activity at 0.0 V (mA/mg-Pt)
7.5% Pt/WC	without CO	377	20.5	136
	with CO	351	19.3	128
20% Pt/C (E-Teck)	without CO	106	28.3	71
	with CO	85	23.5	59

[a] Reprinted with permission from ref 177. Copyright 2008 Elsevier B.V.

methanol.[174,177] They also showed improved resistance to CO poisoning in the hydrogen electrooxidation reaction when compared to that catalyzed by a commercially available Pt/C catalyst. Figure 8 and Table 3 compare the CO tolerance of 20 wt % Pt/C (E-Tek) and 7.5 wt % Pt/WC. It is shown that the current density and ESA value of 20 wt % Pt/C catalyst can be decreased by ca. 20% when 1% CO and 99% H_2 gas were introduced into a 1 M H_2SO_4 electrolyte solution. However, for a 7.5 wt % Pt/WC catalyst, the difference in current density between the presence and absence of CO is only 6−7%.

Using electrochemical half-cell measurements in combination with X-ray photoelectron spectroscopy (XPS) to monitor changes in surface composition, Zellner and Chen[172] confirmed that in an electrochemical environment or exposure to air, W_2C was not stable and immediately oxidized to form surface W_xO_y species, while WC was stable at anode potentials below 0.6 V. Chhina et al.[166] found that the electrochemical stability of WC-supported Pt was still significantly higher than carbon-supported Pt for accelerated oxidation cycling. For a Pt/WC catalyst, WC could be oxidized to a substoichiometric tungsten oxide (WO_x) on the particle surface, which still remained moderately conductive, with little loss in Pt surface area. However, the carbon support is gasified to CO and CO_2 when it is oxidized, causing Pt to be physically disconnected from the carbon support, leading to a low Pt surface area and rapid degradation in fuel cell performance. Additionally, Zhang et al.[178] also made a comparison between W_xC_y-supported Pt and carbon-supported Pt, suggesting that Pt/W_xC_y possessed a higher stability and better cell performance in a fuel cell environment, although its effective catalytic surface area was lower than that of Pt/C.

6. BORIDES

Titanium diboride (TiB_2) as a typical boride is a material of growing interest that is being considered as the base material for a range of technological applications.[179,180] TiB_2 is one of the metal diborides (MB_2, M = Be, Al, Nb, Mo, Ta, Ti, Hf, V, and Cr) and has the same structure as MgB_2. No superconducting phase in the stoichiometric composition was identified during investigations in the 1970s except for metal-deficient diborides of NbB_2.[181] TiB_2 was reported for the first time by Yin et al.[182] as a catalyst support because of its many superior properties such as a high melting point (>3000 °C), exceptional hardness (approximately 25−35 GPa at room temperature, more than 3 times harder than fully hardened structural steel), good electrical conductivity (~10^5 S/cm), high thermal conductivity (~65 W m^{-1} K^{-1}), excellent thermal stability, and corrosion resistance in acidic medium;[183,184] these excellent properties make it a promising support material for PEM fuel cells. This novel catalyst (Pt/TiB_2) was obtained by a colloid route, and highly dispersed Pt nanoparticles on the TiB_2 support were stabilized by Nafion functional polymers. The electrochemical properties of Pt/TiB_2 were investigated by the rotating disk electrode (RDE) technique in a 0.5 M H_2SO_4 electrolyte at 25 °C. It was found that the Pt/TiB_2 catalyst shows a higher reduced current of 0.29 mA cm^{-2} at 0.9 V vs SHE as compared to Pt/C (0.11 mA cm^{-2} at 0.9 V) for the same Pt loading. After 5000 cycles, the Pt/TiB_2 ESA loss rate was 4.08 × 10^{-3} m^2 g^{-1} for every average cycle, whereas the ESA loss rate of the Pt/C was 1.56 × 10^{-2} m^2 g^{-1} for every average cycle. The electrochemical stability of the Pt/TiB_2 catalyst is approximately 4 times higher than that of the commercial Pt/C catalyst, as a result of the support and also possibly from Nafion stabilization effects, which enhanc both the metal−support interaction and the steric hindrance effect of the surface Pt nanoparticles.

7. MESOPOROUS SILICAS

Mesoporous silicas are of great interest for use as electrocatalyst supports in fuel cell applications because they have both a large surface area and uniform hexagonal pores even though their conductivity is low (~10^{-7} S/cm).[185] Using the conventional pore filling impregnation method, Eswaramoorthi and Dalai[36] prepared some SBA-15-supported Pd−Zn nanocatalysts for the production of H_2 from CH_3OH by partial oxidation and steam reforming reactions, in which various amounts of Pd and Zn in the ratio of 1:1.5 were loaded on a calcined SBA-15 support. Table 4 lists the physicochemical characteristics of the Pd−Zn/SBA-15 catalyst and pure SBA-15. As seen in Table 4, SBA-15 has a large surface area of 818 m^2/g, and its average pore diameter is 9.8 nm. The resulting PdZn alloy on the support was found to be stable. Initial results indicate that mesoporous silicas show great promise as a catalyst support for fuel cell applications.

8. ELECTRONICALLY CONDUCTING POLYMERS (ECPS)

Electronically conducting polymers (ECPs) are important materials because of their unique optical, electronic, chemical, and mechanical properties,[186] simple preparation, and feasible application in electrochemical energy conversion. Some polymers such as polyaniline, polypyrrole, and polythiophene have been extensively studied as supports to disperse metallic particles. The physical and chemical properties of these polymers[187−194] are well-known and allow the preparation of electronic conductive polymer-supported electrocatalysts. With reasonable stability over 3 days in acid media such as 1 M hydrochloric acid, these polymer supports provide the possibility of higher surface areas and higher conductivity in the potential range where the organic polymer molecule can be oxidized. Platinum dispersion onto and inside such a polymer support to form supported catalysts can reduce the amount of noble metals used and improve the catalytic activity for the oxidation of hydrogen,[195] small organic molecules such as

Table 4. Physico-chemical Characteristics of PdZn/SBA-15 Catalyst and Pure SBA-15 Support[a]

catalyst	Pd (wt %)	Zn (wt %)	BET surface area (m^2/g)	micropore area (m^2/g)	pore volume (cc/g)	average pore diameter (nm)	CO uptake[b] (μmol/g)	H_2 uptake[b] (μmol/g)
1	0.5	0.75	768	45	1.18	9.7	12.7	8
2	1.5	2.25	683	53	1.02	9.9	19.3	13.7
3	3.0	4.5	596	33	1.15	10.3	26.7	24
4	4.5	6.75	524	21	1.13	10.07	38.2	32
5	5.5	8.25	507	23	1.0	9.9	40.6	35.2
SBA-15			818	95	1.85	10.3		

[a] Reprinted with permission from ref 36. Copyright 2009 Elsevier B.V. [b] Per gram of catalyst.

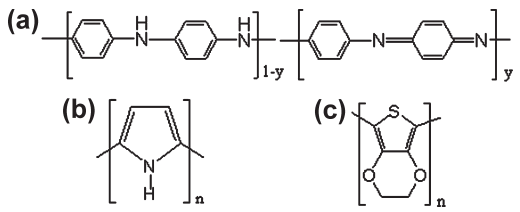

Figure 9. Structures for (a) PANI, (b) PPY, and (c) PEDOT.

formic acid[196,197] and methanol[198−203] by better utilization of the platinum, and, especially, a decreased poisoning effect.[203,204]

8.1. Polyaniline (PANI)

8.1.1. Conventional PANI. Polyaniline (PANI, see Figure 9a) is an attractive material to be used as catalyst support because of its high conductivity in its partially oxidized state[205,206] (e.g., emeraldine, which features an equal number of imine and amine nitrogens in the free-base form, while the polymer is an insulator in the neutralized free-base form). PANI also has high uniformity, and good adhesiveness to some substrates such as carbon nanotubes,[207] glass fiber surfaces,[208] and polystyrene,[209] as well as high chemical stability in aqueous solutions.[210−212] In general, the conductivity levels of neat polyaniline compositions can be as high as 100 S/cm.[213] Polymer blends containing polyaniline compositions have a conductivity range from 10^{-10} to 10^{-1} S/cm (melt processing) and 10 S/cm (solution processing). PANI-supported Pt and Pt alloy catalysts are an effective way to reduce the cost and enhance the efficient use of bulk metals. In general, Pt and Pt alloys can be supported on a PANI support through two main types of procedures: (1) the catalyst particles are incorporated into the polymer film during the electropolymerization of a suitable monomer from a solution containing both monomer and a metallic precursor salt; and (2) the catalyst particles are electrodeposited on a previously prepared polymer film using a solution containing a metallic precursor salt.[214,215] Using the first method, Laborde et al.[204] reported the preparation of Pt-modified polyaniline electrodes. The obtained electrodes showed a higher electrocatalytic activity toward methanol oxidation than bulk platinum electrodes. The poisoning effect was also drastically decreased as proved using in situ electrochemically modulated infrared reflectance spectroscopy (EMIRS) studies. Using the second method, some research groups found that Pt dispersed in the PANI film showed better electro-catalytic activity for electrooxidation reactions such as hydrogen,[216] formic acid,[196,217] CO,[218,219] glycerol,[220] formaldehyde,[221] etc., and the reduction of oxygen,[222] as well as the hydrogen evolution reaction (HER).[223,224] It seems that no matter which method was used, the catalytic activity of the modified electrode was strongly dependent on the catalyst particle size and its distribution onto and inside the polymer film.[225]

To increase the CO and/or methanol tolerance in a direct methanol fuel cell (DMFC), and reduce the usage of expensive Pt metal, Pt alloys were also deposited onto and into the PANI support to form supported catalysts. For example, Hable and Wrighton[226] prepared two PANI-supported alloy electrocatalysts by electrochemical deposition, that is, Pt−Ru/polyaniline and Pt−Sn/polyaniline, repectively. They found that the activity of Pt−Ru/polyaniline catalyst for MeOH or EtOH oxidation was higher than that of polyaniline-coated electrodes modified with Pt alone and that Pt−Ru/polyaniline was more active than the Pt−Sn/polyaniline catalyst. To further improve the activity of PANI-supported Pt−Ru binary catalysts, Lima et al.[227] incorporated a third metal, X (Au, Co, Cu, Fe, Mo, Ni, Sn, or W), to obtain PANI-supported Pt−Ru−X ternary metallic catalysts. A comparative study on the catalytic activities of several ternary alloys toward methanol electrooxidation showed that Pt−Ru−Mo/PANI could not only result in an increase in current density up to 10 times higher than Pt−Ru/PANI in the same potential range but also was very stable at potentials lower than 550 mV vs RHE. By analysis of in situ infrared reflectance spectroscopy,[228] they found that CO_2 was produced from methanol oxidation at 350 mV vs RHE on Pt−Ru−Mo/PANI, which was 100 and 200 mV less negative than that on Pt−Ru/PANI and Pt/PANI catalysts, respectively. Therefore, molybdenum seemed to have the ability to improve the activity of PANI-supported platinum catalyst toward the oxidation of some small organic molecules when it was added into the platinum as an alloy element or a compound.[229−232] Unfortunately, molybdenum and its compounds were not stable and could be dissolved in acidic solutions.[233] Instead of Mo, hydrogen molybdenum bronze (H_xMoO_3)[234,235] was also used to develop a Pt−H_xMoO_3/PANI catalyst for methanol oxidation. This catalyst also showed both improved catalytic activity and stability for methanol oxidation. Regarding other metals such as Os and Pd, Kessler et al.[236] and Grace et al.[237] prepared Pt−Ru−Os/PANI and Pt−Ru−Pd/PANI catalysts. The Pt−Ru−Os/PANI catalyst showed better catalytic activity than that of Pt−Ru−Mo/PANI for the electrooxidation of both adsorbed CO and methanol. In addition, the Pt−Ru−Pd/PANI catalyst showed good activity toward the oxidation of glycerol due to the dispersion of metal nanoparticles onto PANI.

8.1.2. Nanostructured PANI. Nanostructured PANI supports with different morphologies were synthesized using various techniques such as template synthesis,[238] self-assembly,[239] emulsion polymerization,[240] as well as interfacial polymerization.[241] The first attempt to use PANI nanotubes (200 nm outer diameter) as a fuel cell catalyst support showed promising result.[242] In the process, PANI nanotubes, synthesized by a template method on commercially available carbon cloth, were

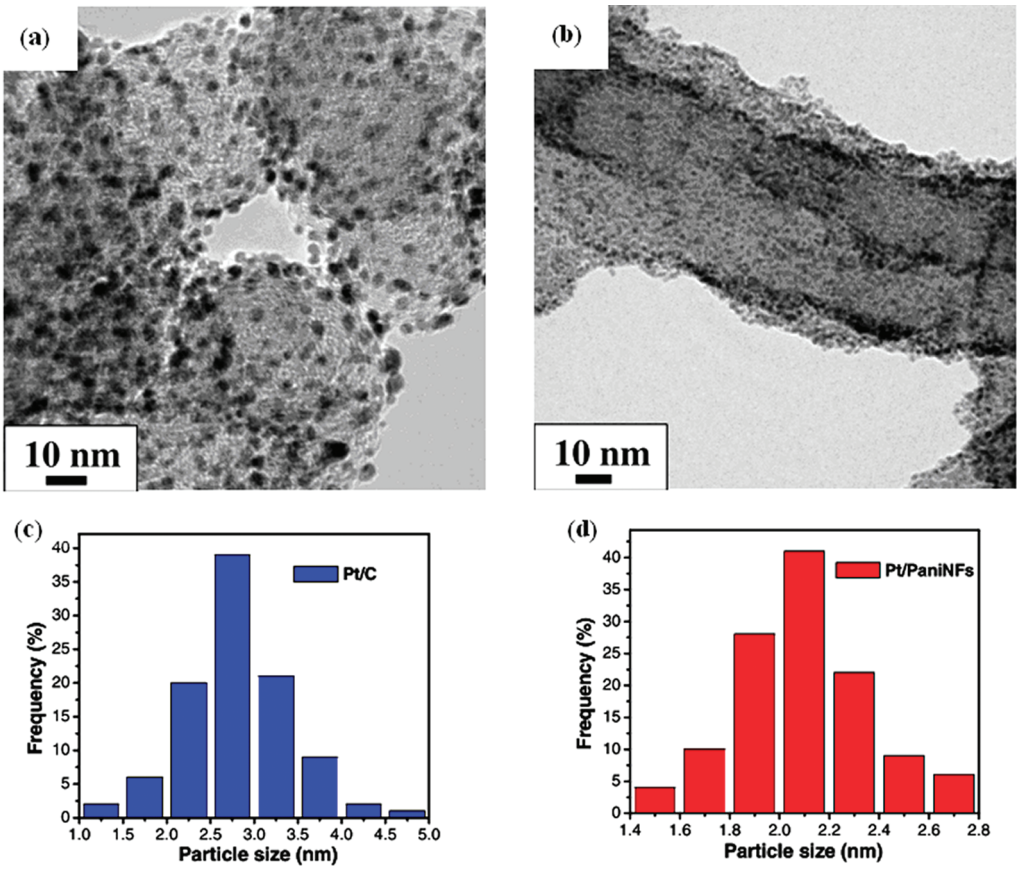

Figure 10. Transmission electron microscope (TEM) images of Pt/C (a) and Pt/PaniNFs (b); histogram of Pt nanoparticle diameter of Pt/C (c) and Pt/PaniNFs (d). Reprinted with permission from ref 244. Copyright 2006 Institute of Physics and IOP Publishing.

used as the catalyst support for Pt particles, and the catalyst obtained was tested for methanol electrooxidation. The results obtained by Rajesh et al.[242] showed that for the template-based Pt/PANI-tubes electrode, the catalytic actvitiy was increased from 10 to 80 mA/cm^2 with increasing Pt loading from 10 to 80 μg/cm^2. However, the catalytic activity was reduced by about 19.0% after 2 h of testing. However, for a conventional Pt/PANI electrode, the catalytic activity was increased from 5 to only 26 mA/cm^2 for the same increase in catalyst loading, and the activity degradation was as high as 75% after 2 h of testing. This is even worse than for a conventional 20 wt % Pt/VulcanXC-72R carbon catalyst, which showed about a 50% activity reduction. So the Pt/PANI-tubes electrode had excellent catalytic activity and stability as compared to both the 20 wt % Pt supported on the VulcanXC 72R carbon and that supported on the conventional polyaniline electrode. The conventional PANI with a granular structure was synthesized by a galvanostatic method (GM), a cyclic voltammetric method (CVM), or a potentostatic method (PM). In 2004, Zhou et al.[243] showed that nanofibular PANI prepared by modified galvanostatic technology, that is, the pulse galvanostatic method (PGM), showed better conductivity and a higher specific surface area than granular PANI, resulting in a considerably higher electrocatalytic activity toward the methanol oxidation reaction. Further development was carried out by Chen et al.[244] and Liu et al.[245] who prepared a PANI nanofiber-supported Pt catalyst and a PANI nanowire-supported Pt catalyst, respectively. They found that nanostructured PANI-supported Pt could give enhanced electrochemical active surface area and improved catalytic activity for methanol oxidation when compared to bulk Pt electrodes. According to XRD and TEM measurements (Figure 10),[244] the supported Pt nanoparticles had an average particle size of 1.5−5 nm with a narrower particle size distribution. Liu et al.[245] found the effective dispersion of Pt particles was about 10−20 nm, and they believed that this particle size range could facilitate the easy access of methanol to the catalytic sites. Being interested, Michel et al.[246] constructed electrodes for fuel cells by sequential spraying. The incorporation of functionalized polyaniline fibers (Pt/PANI-F) in layer-by-layer (LBL) structures gave an enhanced PEM fuel cell performance due to the high conductivity of PANI-F as well as facilitated ion/gas transport through fibrous morphology.

8.1.3. Modification of PANI. Recently, new approaches have focused on the modification of PANI supports for Pt catalyst in an effort to prepare improved electrocatalysts for fuel cells. Regarding the modified structure of PANI supports, two fluorinated polyanilines, that is, poly(2-fluoroaniline) and poly(2,3,5,6-tetrafluoroaniline),[247] were prepared and used as materials for electrocatalytic anodes in bacterial fuel cells. The results showed that some stable fluorinated polyanilines could improve the catalytic activity of platinum toward the oxidation of hydrogen when compared to a conventional polyaniline support.

Considering the support effect of a mixture of polymers, other polymers such as poly(styrene sulfonic acid) (PSS),[248−250] polysulfone (PSF),[251] poly(acrylic acid) (PAA),[252] or Nafion[253,254] were also studied as the second component in a PANI-based support matrix for Pt catalysts. Huang et al.[248] prepared a Pt/PANI-PSS

dx.doi.org/10.1021/cr100060r |*Chem. Rev.* 2011, 111, 7625–7651

catalyst via a doping−dedoping−redoping process. This Pt/PANI-PSS composite electrode exhibited a much higher electrocatalytic activity for methanol oxidation than Pt/PANI. It was thought that the long chains of PSS could align with the chains of conducting PANI to form an aligned configuration, enhancing the mechanical properties of the support matrix and resulting in improved electrochemical stability of the composite electrode.[249] Later, Liu et al.[250] prepared a Pt−Ru/PANI−PSS composite using a different electro-deposition sequence for Pt and Ru. Deposition of Ru before Pt was found to result in a superior electrocatalytic activity for methanol oxidation than that formed by depositing Pt first. Taking into account the advantages of nanostructured PANI, they also prepared a mixed film of polyaniline nanowires (nano-PANI) and PSS and used this as a support for Pt catalysts. The obtained Pt/nano-PANI-PSS catalyst with a spatial distribution of Pt particles showed an improved catalytic activity toward the oxidation of methanol when compared to the conventional Pt/PANI catalyst. In addition to PSS other polymers such as PSF,[251] PAA[252] or Nafion,[253] when used as the second component for a mixed support for Pt catalysts, also showed improved electrocatalytic activity for both the hydrogen and the methanol oxidation reactions. For example, Yang et al.[254] developed a Pt/PANI-Nafion catalyst using a photochemical method for oxygen reduction cathodes. An electrode with a limiting current of 7.6 mA/cm^2 was achieved at a low Pt loading of 14 μg/cm^2, and the total electron transfer number was found to be four.

8.2. Polypyrrole (PPY)

8.2.1. Pure PPY. Polypyrrole (PPY) is a mechanically and chemically stable conducting polymer, and it is easy to prepare. It is permeable to gases and water and exhibits both electronic and ionic conductivities as well.[255] The ionic conductivity of PPY is typically less than 0.1 S/cm in solution and would be expected to be much less than this value in the PPY matrix.[256] However, the electrical conductivity of PPY in the oxidized state can reach up to 500 S/cm under appropriate polymerization conditions.[257] These properties potentially make PPY a feasible catalyst support for PEM fuel cell applications.

Polypyrrole was first synthesized at the beginning of the 20th century[258] (Figure 9b). In 1979, some continuous films of PPY were synthesized by anodic oxidation.[259] Today, there is a tremendous amount of literature on the material properties of this conducting polymer. PPY is considered one of the most attractive conducting polymers to support highly dispersed platinum particles because of its high electronic conductivity (~500 S/cm[256]), porous structure, high stability, and its processability under ambient conditions.[199,260−263] The promoting effect of the PPY support in Pt/PPY catalysts has been confirmed in a number of studies for methanol oxidation.[39,264,265] In addition to improved electrocatalytic activity, Bouzek et al.[266] and Strike et al.[199] also found that PPY-supported Pt catalyst was very stable in H_2SO_4 solution (0.5 or 1 M) containing 1 M MeOH at 25 °C. Beside Pt, PPY can also be modified with other metals including Pd, Pt, Pb, Cu, Ni, Ru, Sn, and Au to produce electrocatalysts.[267,268] Hammache et al.[269] prepared a Cu/PPy catalyst on a Au electrode, which showed a high electrocatalytic activity for methanol oxidation in a DMFC. Chandler and Pletcher[267] studied the effect of PPY films on the kinetics of nucleation and growth of several metals such as Pd, Pt, Pb, and Ru. Sigaud et al.[270] and Trueba et al.[271] also prepared PPY-supported catalysts with some metals such as Pd, Ru, Rh, and Ir.

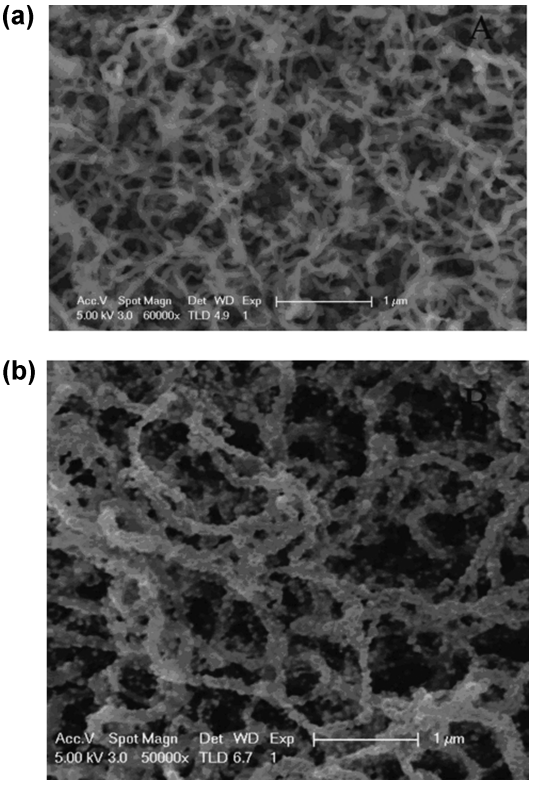

Figure 11. Field emission scanning electron microscopy (FE-SEM) images of the PPY nanowires (a) and the Pt/PPY nanocomposite (b) on bare GCE. Reprinted with permission from ref 272. Copyright 2007 Electrochemical Society.

Their results showed that these electrocatalysts played an important role in improving electrocatalytic activity toward both the hydrogen evolution and the CO_2 reduction reactions. Becerik et al.[261] found that both Pt and Pd supported on PPY showed high catalytic activity for the electrooxidation of D-glucose in neutral media and could reduce the poisoning effect of CO as well.

In addition to connentional PPY films, nanostructured PPY film materials have also attracted special attention, due to their large surface area, high electronic conductivity, and unique charge transport properties. For example, Li and Lin[272] studied the electrocatalytic activity of PPY nanowire/Pt nanocluster composites on a glassy carbon electrode (GCE) toward the ORR as well as the methanol oxidation reaction (MOR), using both cyclic voltammetry (CV) and chrono-amperometry methods. Figure 11 shows the sponge-like matrix of PPY nanowires on the GCE surface with a nanowire diameter of about 60 nm. With the embedding of Pt nanoclusters, the diameter of the PPY nanowires can be expanded to 100−120 nm. This PPY-supported Pt catalyst on an electrode exhibited larger surface area and higher electrocatalytic activities for both the ORR and the MOR than that for a pure Pt modified electrode. This is due to the high dispersion of Pt nanoclusters on a large surface area of PPY nanowires, as well as the synergistic effect of the Pt core and PPy shell.

8.2.2. Modified PPY. For further improvement in both electronic and ionic conductivities, PPY has also been modified by adding a second conductive polymer to form a composite. For example, Qi et al.[255] produced a mixed support of PPY and

polystyrene sulfonate (PSS) for Pt catalyst and tested it as the gas diffusion electrodes (GDE). They observed that the mixed support PPY/PSS had improved electron and proton conductivity and could be used in the process of producing large quantities of standard PEM fuel cell electrodes.[273] Nafion membrane modified by PPY has also been used as a catalyst support. For example, Lee et al.[274] modified Nafion membranes using PPY and used this modified Nafion as the support for Pt deposition. Li et al.[275] employed PPY modified Nafion as a support for Pt catalyst using a similar impregnation method. The membrane electrolyte assembly (MEA) for a DMFC, prepared from this Pt/PPY-Nafion with an anode Pt loading of 0.67 mg cm^{-2} and a cathode Pt loading of 0.56 mg cm^{-2}, showed optimal performance, suggesting a promising method for MEA preparation in DMFC applications. Pt supports based on PPY−Nafion composites have also been used for applications involving microfabricated fuel cells.[276]

8.3. Other Polymers

Besides PANI and PPY, other conducting polymers can also be used as catalyst supports in fuel cell applications. Drillet et al.[277] explored the use of poly(3,4-ethylene-dioxythiophene) (PEDOT) as shown in Figure 9c as a Pt catalyst support for DMFC anodes. It was found that the partially oxidized PEDOT polymer could enhance the catalytic activity of the Pt catalyst for methanol oxidation. This was believed to be due to the change in the morphology of the PEDOT polymer, resulting in an improvement in methanol diffusion within the reaction layer. To investigate the stability of PEDOT-supported Pt catalyst, Drillet et al.[277,278] studied the degradation of PEDOT. Some degradation was noted after electrochemical experiments in 1 M H_2SO_4 solution containing 2 M of CH_3OH at room temperature. Infrared spectroscopy and EDX showed partial decomposition of the thiophene ring and attenuation of the ethylenedioxy group, suggesting that both the sulfur and the oxygen content in the polymer matrix were decreased.[277] In general, PEDOT is a good catalyst support because it has high compatibility with other materials, excellent film forming properties, high conductivity (~200 S/cm in the oxidized state), a high extent of doping, as well as high thermal stability.[279−281] Thermal studies of PEDOT[282,283] showed that continuous degradation only starts to occur at >150 °C and that complete decomposition occurs at >390 °C.

Kuo et al.[279] modified PEDOT using PSS to form PEDOT−PSS support with a network structure for the Pt catalyst (Pt/PEDOT−PSS) when a small amount of Pt particles was embedded into the PEDOT−PSS matrix; a higher electrocatalytic activity toward the oxidation of methanol could be achieved as compared to that catalyzed by a bulk Pt electrode. The PEDOT−PSS matrix provides a pathway for proton migration within the DMFC catalyst layer. Pt alloy catalysts such as Pt−Ru have also been supported on PEDOT−PSS by other researchers.[284,285] As compared to PtRu supported on Vulcan carbon, Arbizzani et al.[284] found that PtRu/PEDOT−PSS catalyst had better stability in lifetime tesing using a DMFC. This polymer-supported catalyst was also tested for both hydrogen and methanol oxidation as well as the oxygen reduction reaction, demonstrating that PEDOT−PSS could be an effective support for both Pt and PtRu catalysts in PEM fuel cells.

Poly(2-hydroxy-3-aminophenazine) (PHAPH) has also been explored as a support for Pt and PtSn catalysts. This polymer is an electrochemically active material with a redox potential around

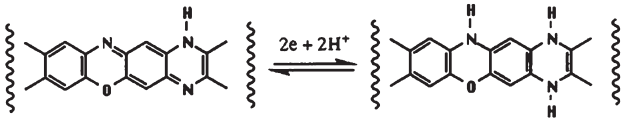

Figure 12. Switching reaction of PHAPH. Reprinted with permission from ref 286. Copyright 1999 Springer.

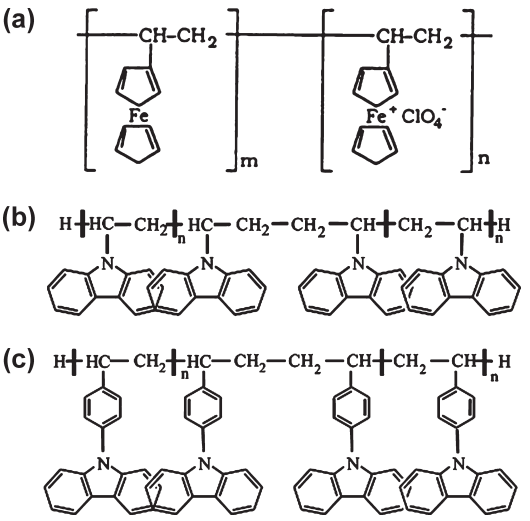

Figure 13. Molecular structures of electronically conducting polymers: (a) electrochemically doped PVF, (b) PVK, and (c) P4VPCz. Reprinted with permission from refs 287 and 288. Copyright 2008 and 2003 Elsevier B.V.

0.1 V vs SHE, as shown in Figure 12. According to Kelaidopoulou et al.,[286] Pt dispersed in PHAPH is much more active than smooth Pt for the electrooxidation of both methanol and formic acid in aqueous perchloric acid solutions. The catalytic activity of the Pt particles could be further enhanced when Sn was codeposited in the PHAPH film. Another polymer, poly(vinylferrocenium) (PVF^+), was also explored as a support material for Pt-based catalysts by Celebi et al.,[287] as shown in Figure 13a for the electrochemically doped PVF. The Pt/PVF^+ catalyst was synthesized by two steps. In the first step, poly(vinylferrocene) (PVF) was electrodeposited at +0.7 V vs Ag/AgCl on the electrode surface by electrooxidizing a 1.0 mg mL^{-1} PVF solution in methylene chloride containing 0.1 M TBAP. In the second step, Pt particles were incorporated into the polymer matrix via cyclic voltammetric scans in an aqueous 2 mM K_2PtCl_4 solution without supporting electrolyte. In addition to poly(vinylferrocenium), Choi et al.[288] have tested two other conducting polymers, poly(*N*-vinyl carbazole) (PVK, see Figure 13b) and poly(9-(4-vinyl-phenyl)carbazole) (P4VPCz, see Figure 13c), as supports for PtRu catalysts for methanol oxidation.

In general, with respect to fuel cell performance, it appears that polymer-supported Pt or PtRu catalysts have less activity as compared to carbon-supported catalysts, particularly for DMFC applications. With respect to this aspect, more effort should be placed on increasing the surface area of the polymer supports. In addition, polymer supports may not be suitable for high temperature PEM fuel cell applications above 100 °C due to serious thermal degradation issues.

9. CONDUCTING METAL OXIDES

Conducting metal oxides are considered to be emerging candidates for catalyst support in fuel cell applications. With reasonable surface area, mechanical strength, thermal, and hydrothermal stabilities, some conducting metal oxides have already been demonstrated as catalyst supports. They have resulted in uniform dispersion of catalyst particles, effective metal−support interactions, as well as reasonable catalytic activities for fuel cell performance.

9.1. Ti,Sn-Based Oxides

9.1.1. Original Ti,Sn-Based Oxides. In recent years, Ti_nO_{2n-1} (where n is between 4 and 10) has attracted attention as a possible electrode material and/or support for electrocatalysts in several applications. In general, there exist several phases in metal oxide structures including the "Magnéli" phase in titanium−oxygen and vanadium−oxygen systems.[289] The Magnéli phases are built up of TiO_6 octahedra, which share corner and edges to form slabs of rutile that can be extended infinitely in two directions. For Ti_nO_{2n-1} structures, there is a homologous "triclinic" phase. The triclinic phase consists of rutile-like layers of TiO_6 octahedra extending indefinitely in the $a-b$ plane and four octahedral thick along the c axis. Among the Ti_nO_{2n-1} series oxides, several oxides exhibit high electrical conductivities at room temperature similar to that of carbon and graphite materials,[290,291] However, these conducting oxides show insignificant catalytic activity for both hydrogen and oxygen evolution[292−294] and are considered more suitable as a catalyst support rather than an electrode or catalyst. Ti_4O_7 and Ti_5O_9, as two compositions of the Ti_nO_{2n-1} series, have proved to be superior materials due to their outstanding combination of high electrical conductivity and high chemical stability in corrosive media such as salt solutions, acid solutions, and alkali liquors. For example, Ti_4O_7, substoichiometric titanium oxide, exhibits the highest electrical conductivity above 10^3 S/cm at room temperature,[290] while the conductivity of Ti_5O_9 is above 10^2 S/cm at room temperature.[295]

Phase-pure microcrystalline Ti_4O_7[296] can be synthesized from TiO_2 by a modified procedure,[294] in which ultrafine rutile TiO_2 was purged with argon in a tube furnace and reduced under H_2 at 1050 °C for 50 min, giving a single-phase Ti_4O_7 powder. This pure Ti_4O_7 powder was used as a catalyst support for several precious metals such as Pt, Ru, and Ir, and the obtained supported catalysts showed both high catalytic activity and stability in fuel cell applications.[296] According to Ioroi et al.,[297] pure Ti_4O_7 support shows a much less anodic corrosion current at voltages >1.0 V vs RHE under PEM fuel cell operating conditions as compared to that of a Vulcan XC-72 carbon support. Furthermore, Ti_4O_7-supported Pt electrocatalyst shows comparable specific activities for both the hydrogen oxidation reaction (HOR) and the oxygen reduction reaction (ORR) as compared to a conventional carbon-supported Pt catalyst at 80 °C under fuel cell operating conditions. To evaluate both HOR and ORR activities, membrane electrode assemblies (MEAs) with Nafion 112 membrane were prepared, and the single cell performances (H_2/O_2, 80 °C, atmospheric pressure) with these MEAs were examined. Later, in a high-potential stability test (1 h at an anodic potential of 1.0−1.5 V vs RHE), Ioroi et al.[298] demonstrated a significant improvement in catalyst stability when Pt/Ti_4O_7 was used as a catalyst as compared to Pt/XC72 catalyst. The change of electrochemically active area (ECA) with holding potential shown in Figure 14 indicates that Pt/Ti_4O_7 catalyst is stable within the potential range examined, whereas 30% Pt/XC72-HTT catalyst is not stable when the potential is higher than 1.3 V. The instability of the Pt/XC72-HTT catalyst was thought to be mainly due to carbon corrosion in the catalyst layer. A single cell using a Pt/Ti_4O_7 cathode catalyst was also constructed and tested at 80 °C using H_2/O_2 for 350 h and validated the stability of the metal oxide-supported catalyst.

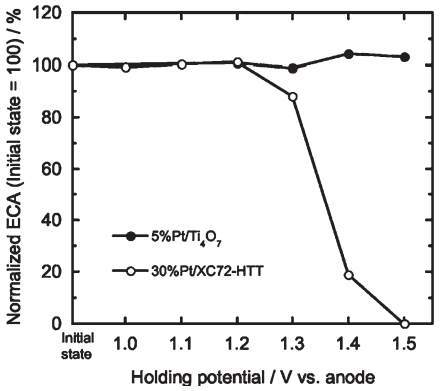

Figure 14. Normalized ECA versus holding-potential plots for 5% Pt/Ti_4O_7 and 30% Pt/XC72-HTT cathodes bonded to N115 membrane. Reprinted with permission from ref 298. Copyright 2008 The Electrochemical Society.

As compared to pure Ti_4O_7, Ebonex, a commercial product (Atraverda Ltd., Sheffield, UK), is an electrically conductive ceramic composite with several reduced titanium oxide phases consisting mainly of Ti_4O_7 and Ti_5O_9.[299] This commercial metal oxide was also explored as a catalyst support. For example, Pollock et al.[300] attempted to add ruthenium or platinum to the surface of Ebonex to form catalysts. However, although Ebonex had high conductivity and good chemical and mechanical stability, the electron transfer reactions were reported to be very slow on its surface.[301−303] Fortunately, this material has a porous microrough surface, which favors the deposition of metal. For example, Ebonex-supported metal was shown to have good quality and adhesive deposits, and as a result the kinetics were similar to those on bulk metal.[301,304] Farndon et al.[305] discussed the surface interaction between the Pt particle and the as-supplied Ebonex support. A number of researchers[281,298,306] have suggested that Ebonex could interact with the deposited metal to change the catalytic activity, and this was confirmed by Slavcheva et al.[307] They synthesized Pt and PtCo nanoparticles supported on Ebonex by the borohydride reduction method. Because of the metal−support interactions, the PtCo/Ebonex catalyst was shown to facilitate the oxygen evolution reaction, which started at lower overpotentials. For the oxygen reduction reaction, this PtCo/Ebonex catalyst gave a higher reaction rate than those catalyzed by either Pt/Ebonex or bare PtCo catalysts. According to Vracar et al.,[306] the Pt/Ebonex catalyst showed a significant enhancement in the catalyzed oxygen reduction reaction compared with polycrystalline Pt. This result was believed to come from the interactions of Pt nanoparticles with Ebonex support as well as the d-band coupling mechnism where the surface reactivity is given by the energy shift of the surface d-states with respect to the Fermi level. Additionally, Farndon et al.[290] and Chen et al.[296] investigated the electrochemical stability of Pt/Ebonex catalyst in alkaline and acidic media, respectively. The results showed that Pt/Ebonex-catalyzed electrodes with a Pt loading

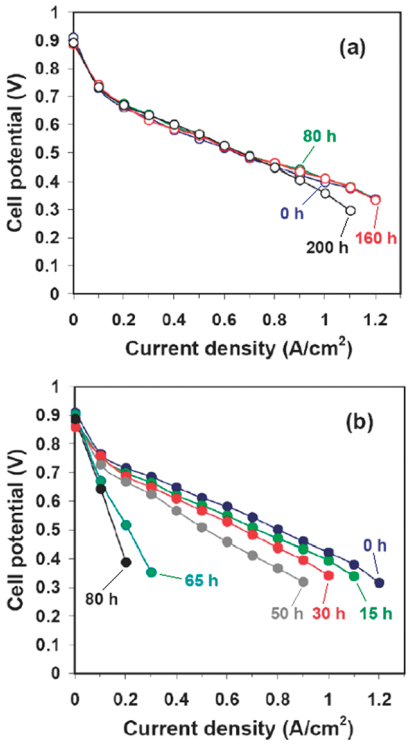

Figure 15. Polarization curves for PEM fuel cells with (a) Pt/TiO_2 and (b) Pt/C electrocatalysts after the potential was held according to the AST protocol for 0−200 and 0−80 h, respectively. The Pt loading was 0.5 mg/cm^2 on the anodic side (LT140EW, BASF) and 0.4 mg/cm^2 on the cathodic side. Reprinted with permission from ref 308. Copyright 2009 Wiley Interscience.

of 2 mg/cm^2 were stable in a flow electrolysis cell (1 M NaOH) for 500 h. Unfortunately, the Pt/Ebonex catalyst had a short-lived electrochemical stability under conditions of oxygen evolution in an acidic solution (0.5 M H_2SO_4).

In recent work,[308] Huang et al. focused extensively on the improvement of fuel cell reliability and durability using TiO_2-supported Pt catalyst (Pt/TiO_2), although TiO_2 had low electrical conductivity. Considering the nonconductive materials as a catalyst support, they used pluronic P123 as a surfactant to prepare porous TiO_2 via a template-assisted route. They obtained the Pt/TiO_2 electrocatalyst by mixing porous TiO_2, $NaBH_4$, H_2PtCl_6, and sodium dodecyl sulfate. Their results showed Pt/TiO_2 exhibted more electrochemical stability and performance than Pt/C. Figure 15 shows the polarization curves for the Pt/TiO_2 and Pt/C electrocatalysts after the potential was held at 1.2 V for 0−200 and 0−80 h, respectively. The polarization curves for Pt/TiO_2 were similar even after a corrosion time (T_c) of 200 h, while Pt/C showed a significant decrease in performance after T_c = 50 h due to carbon corrosion and subsequent detachment and agglomeration. Table 5 summarizes the size of the Pt particles and the electrochemical surface area (ECSA) for two Pt electrocatalysts at T_c = 0 and 80 h. Clearly, a 4-fold increase in the particle size (d_{Pt} = 11.5 nm) relative to the initial value (d_{Pt} = 2.5 nm) was observed for Pt/C due to carbon corrosion and migration and agglomeration of Pt particles. As shown in Figure 16, electrochemical corrosion is one of the most important issues that affects the long-term stability of PEM fuel cells. In the case of Pt/TiO_2, however, there was only a slight increase of the Pt particle size, suggesting the ultrahigh stability of

Table 5. Particle Size (d_{Pt}) and Electrochemical Surface Area (ECSA) Measured for Two Pt Electrocatalysts after the Potential Was Held at 1.2 V for 0 and 80 h[a]

	d_{pt} (nm)		ECSA (m^2/g)	
catalyst	0 h	80 h	0 h	80 h
Pt/TiO_2	6.2	7.8	13.8	11.0
Pt/C	2.5	11.5	53.1	3.8

[a] Reprinted with permission from ref 308. Copyright 2009 Wiley interscience.

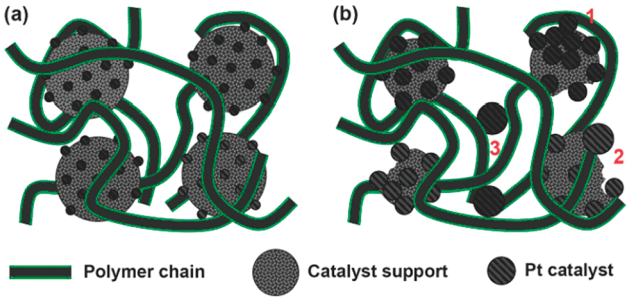

Figure 16. Schematic representation of the effect of carbon corrosion on (1) agglomeration, (2) coalescence, and (3) loss of Pt particles in the membrane electrode assembly (MEA) during operation of PEM fuel cells: (a) normal (corrosion-resistant) electrode and (b) corroded electrode. Reprinted with permission from ref 308. Copyright 2009 American Chemical Society.

the Pt/TiO_2 support at high positive potentials. The stability can be attributed to the strong metal support interaction between the Pt particles and TiO_2 support. It has been reported that TiO_2 can anchor the Pt particles by interacting with Pt, thereby inhibiting Pt migration and agglomeration.[309] Sanchez et al.[310] prepared Pt/TiO_2 catalyst via a one-step synthesis method. They directly mixed a Pt precursor, platinum acetylacetonate, with $Ti(OBut)_4$ at a pH of 3, and then dried the product at different temperatures, such as 70, 200, 400, 600, and 800 °C. They obtained the Pt/TiO_2 electrocatalyst without reducing the sample in hydrogen. X-ray analysis showed that there were three nanophases: rutile (the majority phase), anatase, and platinum. From the Rietveld refinement of the crystalline structure of these phases, a platinum weight concentration equal to its nominal value was determined with most platinum segregated forming metallic platinum. Importantly, it was concluded that platinum can promote the formation of the rutile phase, even at a platinum concentration as low as 0.1 wt %. Unfortunately, they did not measure the electrochemical properties of the synthesized electrocatalysts.

Beside Ti-based oxide-supported catalysts, SnO_2-supported metal catalysts have also been investigated.[311−313] It was demonstrated that platinized tin oxide surfaces can give a high catalytic activity for methanol electrooxidation.[311−313] For example, Sekizawa et al.[314] prepared a SnO_2-supported Pd catalyst and found that the Pd/SnO_2 catalyst enhanced the catalytic activity toward methanol oxidation. It was believed that the existence of an interaction between the palladium and SnO_2 support material as well as high dispersion of the active sites were responsible for this activity enhancement. Furthermore, SnO_2-supported Pt or Pd was also found to be effective in the oxidation of CO.[315−317] Okanishi et al.[318] emphasized the interaction between platinum

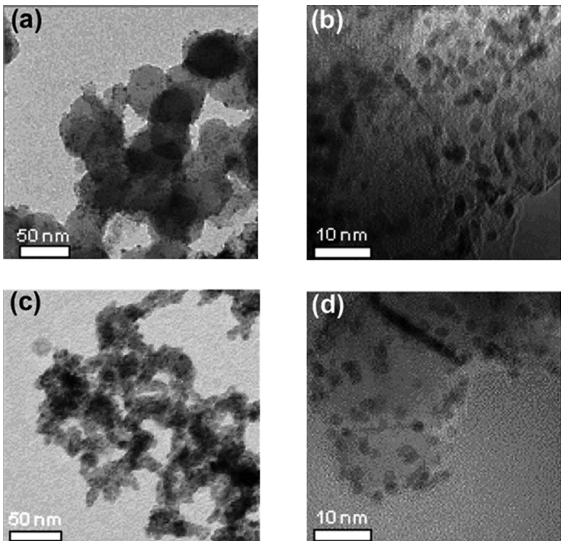

Figure 17. Transmission electron micrograph (TEM) images of Vulcan XC-72 (a and b) and Nb-TiO_2 (c and d)-supported Pt catalysts. Reprinted with permission from ref 320. Copyright 2007 Elsevier B.V.

and tin oxide using a conventional Pt/C catalyst for comparison. They found that both catalysts degraded in the presence of CO in hydrogen. In the presence of 100 ppm CO in H_2, the anode hydrogen reaction can be significantly depressed if Pt/C catalyst is used. However, if Pt/SnO_2 catalyst is used, this depression becomes much smaller, indicating that Pt/SnO_2 catalyst is a CO tolerant catalyst. Baker et al.[319] studied gold nanoparticles supported on hydrous tin−oxide (Au/SnO_x) and described strategies for optimizing catalyst preparation and oxygen reduction reaction electroactivity. Again, the interaction between the metal and SnO_x was claimed to be responsible for a high catalytic activity for the four-electron oxygen reduction reaction in an acid electrolyte.

9.1.2. Metal-Doped Oxides. As discussed previously, titanium oxides are promising as catalyst supports due to their stability in fuel cell operation atmosphere, low cost, commercial availability, stability in water, and the ability to control their size and structure.[320] As their precursor, TiO_2, one of the semiconductors, has been explored as a catalyst support. To increase its electronic conductivity, doping strategies have been developed using Nb and Ru, respectively.[321,322] Using hydrothermal synthesis, Park and Seol[320] prepared a Nb doped TiO_2 nanostructure support and synthesized Pt-based catalyst using this support material for the oxygen reduction reaction. They found that the formed catalyst (Pt/Nb−TiO_2) had well-dispersed Pt particles with an average size of ∼3 nm supported on Nb−TiO_2 nanostructure supports with a particle size of ∼10 nm, as shown in Figure 17. As compared to carbon-supported Pt catalyst, the Pt/Nb−TiO_2 catalyst showed an excellent oxygen reduction reaction activity due to the strong interaction between the oxide support and the metal catalyst. Garcia et al.[323] tested PtRu alloy catalyst supported on Nb doped anatase TiO_2 support (i.e., $Nb_{0.1}Ti_{0.9}O_2$) and found that this PtRu/$Nb_{0.1}Ti_{0.9}O_2$ catalyst was electrically conductive and had reasonable activity toward methanol oxidation. Chen et al.[296] reported that the $Nb_{0.1}Ti_{0.9}O_2$ support had electronic conductivity in the range of 0.2−1.5 S/cm. Although the electrochemically active surface area of the commercially available PtRu/C was slightly higher than PtRu/$Nb_{0.1}Ti_{0.9}O_2$, the catalyst current per active site of PtRu/$Nb_{0.1}Ti_{0.9}O_2$ catalyst was higher than the PtRu/C catalyst. Chen et al.[324] synthesized $Ti_{0.9}Nb_{0.1}O_2$, a doped rutile compound, and used it as a support for mixed metal catalysts containing Pt, Ir, Ru, Os, and Rh. Because of its nondefective oxygen lattice, $Ti_{0.9}Nb_{0.1}O_2$ was found to be more electrochemically stable than both Ebonex and Ti_4O_7.

For a Ru doped TiO_2 ($Ru_xTi_{1-x}O_2$) support, Haas et al.[322] found that the conductivity of the support could be increased with increasing ruthenium mole fraction, with a content greater than 27% required for good conductivity. The mixed oxides with a particles size of about 200 nm were prepared using a sol−gel routine, and Pt was deposited on this support using a chemical deposition process. In a half-cell configuration containing 0.5 M phosphoric acid electrolyte, cyclic voltammetry results showed that the Ru doped TiO_2 support for Pt catalyst had an active platinum surface area comparable to that of commercially available carbon-supported Pt catalysts. To further improve the electrochemical properties of the Ru doped TiO_2 support, Wang et al.[324] synthesized a $Ru_{0.1}Ti_{0.9}O_2$ nanopowder using TiN nanoparticles and $RuCl_3$ precursors by the impregnation-thermal decomposition method, and then deposited Pt nanoparticles on the surface of this support to form $Ru_{0.1}Ti_{0.9}O_2$ catalyst. Fuel cell testing using this catalyst in the cathode catalyst layer showed fairly high catalyst performance and stability.

Besides TiO_2, SnO_2 has also been explored as a support for electrocatalysts. Although SnO_2 itself is a poor electrical conductor, doping SnO_2 using some metals such as Sb and Ru can significantly increase the electrical conductivity, making it possible to use as a catalyst support. According to Lee et al.,[325] the Sb doped SnO_2 can exhibit a conductivity around 0.11 S/cm at room temperature, and the conductivity of the Ru-doped SnO_2 film is about 2.5×10^{-3} S/cm.[326] Besides the large surface area of such a supported catalyst, the doping metals such as Sb also have beneficial effects such as OH species adsorption and electronic effects for improving the electroxidation of small alcohols.[307] Santos et al.[327] investigated the electrooxidation of methanol on Pt microparticles dispersed on Sb−SnO_2 thin films. The Sb doped SnO_2 films were found to be effective for the dispersion of Pt microparticles due to their high roughness. Experiments showed that Sb−SnO_2-supported Pt catalyst exhibited a large intrinsic electrocatalytical activity for methanol electrooxidation due to factors such as a structural effect promoting high dispersion of Pt and the nature of the oxide film favoring electrooxidation, and possibly the bifunctional mechanism. Lee et al.[325] also deposited Pt colloidal particles on Sb-doped SnO_2 (antimony doped tin oxide, ATO) nanoparticles with various amounts of Pt loading. Typical polycrystalline diffraction patterns for these Pt/ATO catalysts are shown in Figure 18, indicating that the Sn ions are replaced by Sb in the cassiterite SiO_2 ploycrystal structure without forming any new phases of Sb compounds. The size of the ATO nanoparticles calculated from the (110) peak using Scherrer's equation was ∼5.2 nm. These catalysts were tested for both methanol and ethanol electrooxidation, and it was found that their catalytic activities were enhanced when compared to that of a Pt/C catalyst. In addition, Pt/ATO catalyst also exhibited a much higher electrochemical and thermal stability than the Pt/C catalyst, when tested using direct alcohol fuel cells. Besides Sb, Ru was also used as a doping metal for SnO_2. Pang et al.[328] prepared some Ru-doped SnO_2 nanoparticles by chemical precipitation and calcinations at 823 K. Ru-doped SnO_2 nanoparticles were found to have high stability in dilute acidic

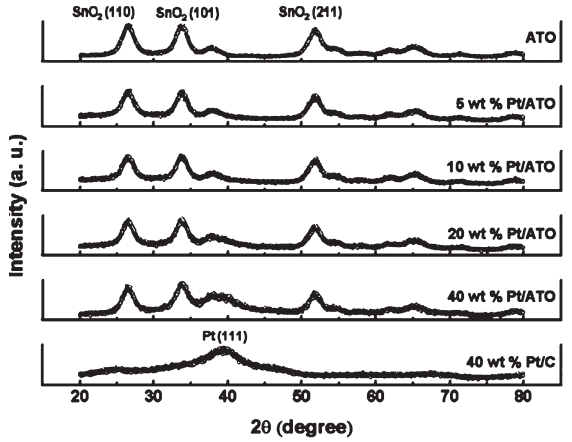

Figure 18. XRD patterns of the ATO support and the prepared electrocatalysts. Reprinted with permission from ref 325. Copyright 2008 Elsevier B.V.

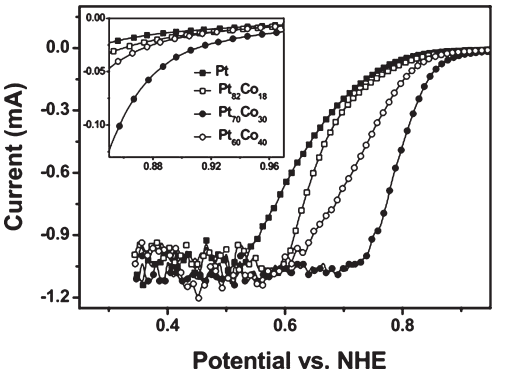

Figure 19. Typical ORR curves on PtCo/TONT with different ratios of Pt to Co in O_2 saturated 0.5 M $HClO_4$ electrolyte with a scan rate of 5 mV/s. Reprinted with permission from ref 337. Copyright 2008 The Electrochemical Society.

solution. As compared to the Pt/SnO_2 catalyst, the $Pt/Ru-SnO_2$ catalyst showed both improved electrocatalytic activity and stability. It was also found that the optimal atomic ratio of Ru to Sn in Ru-doped SnO_2 materials is 1/75.

9.1.3. Nanostructured Oxides. It is well-known that inorganic oxide materials with a one-dimensional (1D) structure (i.e., nanowire, nanorod, nanotube, and nanofibers) have unique physicochemical properties such as one-dimensionality, a crystalline phase state, nonlinear optical properties, quantum size effects, hollow core structures, very large specific surface areas, narrow inner pores, and active catalytic surfaces.[329−331]

Such materials have a wide range of applications including catalysis.[332] For example, titanium dioxide nanotubes (TONTs) have been explored as a catalyst support[333] because of their open mesoporous morphology and high specific surface area. It is believed that the semiconducting properties of TONTs can result in a strong electronic interaction between the support and catalyst, improving the catalytic activity for electrochemical reactions. This propertiy plus the moderate electrical conductivity of these nanotubes make them attractive for catalyst applications in the PEM fuel cell catalysts. For example, Wang et al.[334] and Macak et al.[335] found that TiO_2 nanotube-supported Pd catalyst showed excellent catalytic activity for methanol oxidation. In their research, conventional TiO_2 nanoparticles with an average particle size of 10 nm and TiO_2 nanotubes with a 10 nm diameters were used as the supports for Pd catalysts. The Pd/nanotube$-TiO_2$ catalyst displayed a catalytic activity superior to those of both pure Pd and conventional TiO_2 nanoparticle-supported Pd catalysts. When bimetallic Pt−Ru nanoparticles were dispersed over a nanotubular self-organized TiO_2 matrix, Macak et al.[335] found that the overall electrocatalytic activity was strongly dependent on the morphology of the support. In addition, TONTs have been explored as a catalyst support for the oxygen reduction reaction. For example, Kang et al.[336] developed some TONT arrays by electrochemical anodization and used them as supports for Pt and alloyed Pt−Ni catalysts. As compared to the as-deposited PtNi/TONT, annealed PtNi/TONT catalyst showed a higher oxygen reduction reaction activity. They believed that the d-electronic structure of Pt could be modified by the formation of the Pt−Ni alloy catalyst, leading to a favorable adsorption of O_2. Furthermore, when the as-prepared catalyst was heat-treated, a strong metal−support interaction effect could be observed, which might be associated with electron transfer from the oxide support to the metal. Here, the interaction means that the d-electron configuration of the Pt particle can be modified upon its deposition on the support. This effect was detected by the X-ray photoemission spectroscopy (XPS) spectra and was found to favor ORR activity. Kang et al.[337] also sputtered PtCo catalysts on TiO_2 nanotube arrays to form catalysts with different Co contents. Figure 19 shows typical oxygen reduction curves for different compositions of PtCo/TONT with 30% (atomic) of Co showing the best activity with a positive shift in the onset potential of 200 mV.

SnO_2 has also been found to exhibit other nanostructures such as belts/ribbons, wires, and networks. In particular, SnO_2 nanowires (NWs) as a one-dimensional nanomaterial have demonstrated electrical, optical, mechanical, and thermal properties superior to those of the traditional bulk materials. Among various kinds of nanowires, SnO_2 NWs have several unique advantages as supports for dispersing noble metal nanoparticles such as Pt. By a thermal evaporation method, Saha et al.[338] developed SnO_2 NWs and dispersed these NWs on the carbon fibers of carbon paper. After that, they electrochemically deposited Pt nanoparticles onto the surface of the SnO_2 NWs to form a catalyzed electrode. In comparison with a standard Pt/C electrode, this composite Pt/SnO_2 electrode exhibited a higher electrocatalytic activity for both the oxygen reduction reaction and the methanol oxidation reaction. The same researchers also[339] prepared a composite electrode using Pt−Ru catalyst supported on SnO_2 nanowires for electrocatalytic oxidation of methanol. Their results showed both high mass and specific activities for methanol oxidation and CO tolerance. In general, these methods for fabricating electrodes have provided a new route to make metal oxide NWs-based catalyst supports for PEM fuel cell applications.

9.2. Tungsten Oxides (WO_x)

9.2.1. Pure WO_x. Tungsten oxides (WO_x), a commercially available material, are often used as conducting oxides for smart windows. Tungsten oxides are an n-type semiconductor with a band gap of about 2.6−2.8 eV.[340] Because of the oxidation states from 2 to 6 on the tungsten side, they can have many forms for various applications in electrochemical fields.[341] For fuel cell applications, tungsten oxides have been explored as potential noncarbon catalyst supports, such as Pt-based catalysts supported on sodium tungsten bronze (Na_xWO_3) for phosphoric

dx.doi.org/10.1021/cr100060r |Chem. Rev. 2011, 111, 7625–7651

acid fuel cells (PAFCs).[342,343] Because of the formation of a phosphotungstate complex, this catalyst appears to be unsuccessful. However, when tungsten oxide was used as a catalyst support in DMFCs,[344] the formed Pt/WO_x catalyst showed much higher catalytic activity toward methanol oxidation. This activity enhancement was believed to be due to the formation of tungsten bronzes, which favor the dehydrogenation of methanol. In addition, the oxophilic nature of the oxide support may also help in removing the adsorbed intermediates during the methanol oxidation.[345] The enhancement effect in methanol eletro-oxidation was believed to be due to the synergistic interaction between Pt and WO_x because this interaction can lead to the best CO_{ads} tolerance if methanol electrooxidation proceeds via CO_{ads} species.[346,347] To evaluate CO tolerance of the Pt/WO_x catalyst, Micoud et al.[348] prepared a well-defined WO_3-supported platinum catalyst (Pt/WO_x) using the impregnation-reduction method in which a platinum salt was reduced to Pt nanoparticles and then dispersed onto commercially available monoclinic WO_3 support. By monitoring CO_{ads} electrooxidation currents at potentials as low as 0.1 V vs RHE, they demonstrated that Pt/WO_x catalyst had a higher CO tolerance than that of carbon-supported Pt or PtRu catalysts. In addition, it has also been found that tungsten oxides can help the proton transfer process during methanol electrooxidation due to the formation of tungsten trioxide hydrates.[349,350] Park et al.[351] observed these effects for methanol electrooxidation catalyzed by a PtRu−WO_3 catalyst.

In general, Pt loading on metal oxide supports is one of the important controlling factors for catalytic activity enhancement. Reducing Pt loading without compromising the catalyst activity is always desired in terms of catalyst cost reduction. However, for WO_3-supported Pt catalysts, when Pt loading was greater than 50 wt %, the catalytic activity for methanol electrooxidation could be as high as that of a pure Pt catalyst consisting of spherical Pt particles with particle sizes ranging between 50 and 150 nm.[352]

For WO_3-supported Pt catalysts, the morphology and structure of the WO_3 support were found to be quite important in the preparation of active Pt catalysts for methanol electrooxidation. For example, Ganesan and Lee[353] prepared WO_3 microspheres as a Pt catalyst support, and the obtained catalyst showed higher stable electrocatalytic activity for methanol oxidation as compared to that for commercially available 20 wt % PtRu/Vulcan-XC72 and 20 wt % PtRu/carbon-microspheres catalysts. Cui et al.[344] synthesized Pt catalyst supported on mesoporous WO_3 particles. This mesoporous WO_3 support had a high surface area, ordered pore structure, and nanosized wall thickness of about 6−7 nm. Figure 20 shows typical TEM images of this support. It can be seen that WO_3 possesses a well-ordered mesoporous framework in the (111) and (100) directions of cubic *Ia*3*d* symmetry, which is a replica of the mesoporous structure of the silica template, KIT-6. The energy-dispersive X-ray spectra (EDS) pattern shown in Figure 20c proves that the silica template was completely removed. The selected area electron diffraction (SAED) pattern (Figure 20d) indicates that the m-WO_3 replica is well crystallized and has a polycrystalline character. This Pt catalyst supported on mesoporous WO_3 was tested for methanol electrooxidation, and the results showed that the electrocatalytic activity of 20 wt % Pt/WO_3 was significantly higher than that of the commercially avaialble 20 wt % Pt/C catalyst and was comparable to that of 20 wt % PtRu/C catalyst in the potential region of 0.5−0.7 V vs NHE. In addition, Barczuk et al.[354] immobilized the same amount of PtRu catalyst on three different WO_3 matrices to form supported catalysts. The obtained

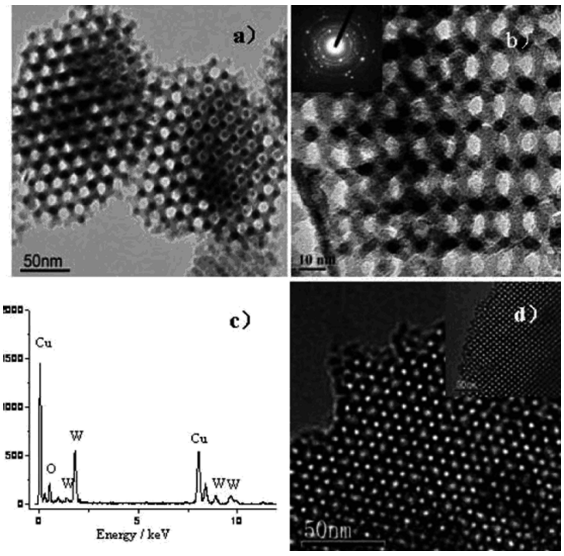

Figure 20. TEM images (a,b) of WO_3 in (111) and (100) directions, respectively, with SAED pattern of WO_3 as the inset in part b; EDS pattern of m-WO_3 (c); TEM images of KIT-6 (d) in (111) direction and in (100) direction (inset in d). Reprinted with permission from ref 344. Copyright 2008 American Chemical Society.

catalysts with both nanoporous and microporous WO_3 matrices as supports had high surface areas and significantly enhanced electrocatalytic activity toward methanol oxidation as well.

Tungsten oxides as a Pt catalyst supports can also promote the oxygen reduction reaction. For example, Chhina et al.[341] showed that the oxygen reduction activity of Pt/WO_3 catalyst remains high, even after accelerated oxidation tests in deoxygenated 0.5 M H_2SO_4 at 30 and 80 °C, respectively, while activity was extremely degraded after the same accelerated oxidation tests with a commercially available carbon-supported Pt catalyst (Hispec 4000). Moreover, tungsten oxide was claimed to be not only more thermally stable against oxidation than Vulcan XC-72R but also extremely stable under the electrochemical oxidation conditions at 30 °C. With respect to stability, McLeod and Birss[355] also evaluated Pt/WO_x films as methanol exlectrooxidation catalysts. Using the sol−gel method, they synthesized two types of WO_x, using ethanol (Type 1) or water (Type 2) as the solvent, respectively. Although both types of WO_x exhibited a low resistance, which is a necessary property for a fuel cell catalyst support, Type 2 films showed more stable methanol oxidation currents than did Type 1 films. This was believed to be due to the loss of WO_x from the Type 1 film. Therefore, WO_x produced via the Type 2 synthesis seemed to be more promising as fuel cell catalyst support than Type 1 WO_x. Although a Pt/WO_x catalyst usually exhibits high stability, tungsten dissolution has still been observed in acid media,[356] which is an issue for PEM fuel cell applications. To improve the chemical stability of WO_3 in acid media, Raghuveer and Viswanathan[357] attempted to use suitable Ti^{4+} substitution in the WO_3 framework. It was found that the stability of WO_3 in an acid medium could be significantly improved when a small amount of Ti^{4+} was put into the framework. Unfortunately, Ti^{4+} substitution can increase the ohmic resistance of the WO_3 framework.

9.2.2. WO_3 Nanorods. One-dimensional (1D) nanorods of WO_3 have been explored for use as catalyst supports in electrocatalyst applications. The results have demonstrated that the deposition of Pt nanoparticles on the WO_3 nanorods can

generate large specific surface areas and prevent agglomeration of Pt nanoparticles. In particular, 1D WO_3 nanorod-supported Pt catalyst can have a strong synergetic effect, which improves the kinetics of methanol oxidation. Rajeswari et al.[358] prepared WO_3 nanorods by simply pyrolyzing surfactant encapsulating tungsten oxide clusters. The obtained nanorods with a length of 130−480 nm and a width of 18−56 nm were used as the supports for Pt catalyst. The formed catalyst was tested for methanol oxidation and demonstrated both comparable catalytic activity and stability to commercially available 20% Pt−Ru/C catalyst. Maiyalagan and Viswanathan[359] employed a simple template synthesis method to develop WO_3 nanorods with a 200 nm size by directly calcinating phosphotungstic acid in the channels of an alumina template. Pt particles were then dispersed on these WO_3 nanorods to form Pt/WO_3 catalyst. A glassy carbon electrode coated with this Pt/WO_3 catalyst showed high eletrocatalytic activity for methanol oxidation and was used to study the synergistic effect between Pt and WO_3.

9.3. Sulfated Oxides (S−ZrO_2)

Sulfated zirconium oxides (S−ZrO_2) have also been explored as catalyst supports for many chemical reactions.[359,360] Normally, the ZrO_2 structure has monoclinic and tetragonal crystalline phases.[312] These phases sometimes give different physical and/or chemical properties, and therefore different catalytic activities when used as a catalyst support. However, after modification by sulfonation to form S−ZrO_2, a solid superacid, the S−ZrO_2 gave superior catalytic activity in many reactions.[360,361] For example, Hara and Miyayama[362] employed different synthesis methods and synthesized three desired sulfonated zirconia (S−ZrO_2) samples. They found that the electronic polarization induced by such SO_x modification could improve the Lewis and Brønsted acidities on Zr, leading to higher proton conductivities. This electronic polarization (resonant process) occurs in a neutral atom when the electric field displaces the electron density relative to the nucleus it surrounds. All of the S−ZrO_2 samples showed strong bonding between SO_x and Zr on a heat-treated S−ZrO_2 surface. Waqif et al.[363] tested the stability of sulfated samples at various temperatures in the presence of methanol and water. S−ZrO_2 was found to retain a high activity at 300 °C for the dehydration of methanol. When used in fuel cells, sulfated zirconia-supported Pt catalyst gave a high cell performance.[364,365] As compared to Pt/C, Pt/S−ZrO_2 can provide proton conductivity to help catalytic processes and improve fuel cell performance. Also, the content of the Nafion ionomer in the catalyst layer may be able to be reduced if using S−ZrO_2 as the support.

For example, Suzuki et al.[364] synthesized sulfated zirconia-supported Pt (Pt/S−ZrO_2) using ultrasonic spray pyrolysis (USP). They found that Pt was dispersed on the S−ZrO_2 surface as nanoparticles with a diameter of ∼8 nm. The cell performance of Pt/S−ZrO_2 cathode was higher than that of Pt/C if both of the catalyst layers were not impregnated with Nafion ionomer. This indicates that the Pt/S−ZrO_2 catalyst could reduce the usage of Nafion ionomer in the catalysts layer. USP is one of the one-step synthesis methods to directly prepare some materials like metal oxides-supported metal electrocatalyst with high surface area support. Recently, USP has been also demonstrated as a facile and novel method to prepare meso- and macroporous supports including carbon for electrocatalysts.[366] In a typical USP procedure as shown in Figure 21, a humidifier ultrasonically nebulizes a precursor solution producing a mist of micrometer-sized droplets. The aerosol droplets are then carried by argon gas

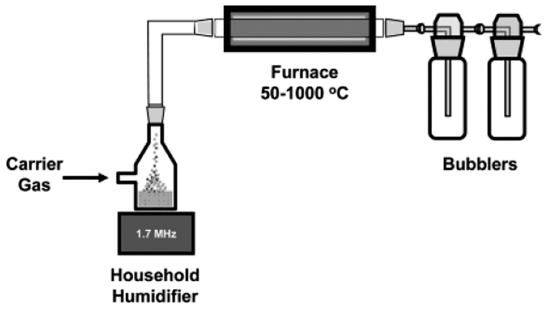

Figure 21. Ultrasonic spray pyrolysis (USP) experimental apparatus. Reprinted with permission from ref 367. Copyright 2007 American Chemical Society.

into a furnace where solvent evaporation and precursor decomposition occur. Bubblers collect the support, and byproducts remain dissolved in the bubbler collection solvent or are flushed out of the system by the carrier gas.[367] Theoretical studies[368] indicate that the solubility of the precursor is very important for the direct preparation of some material-supported metal electrocatalysts. If the difference in precursor solubility is large, then the solute of lower solubility will precipitate first. Depending on whether the particle can continue to shrink, the other solutes will segregate to its surface where they will heterogeneously nucleate. The composite particle will consist of relatively larger crystallites of the first phase surrounded by smaller crystallites of the second phase.

Zhang et al.[365] synthesized a self-humidifying membrane based on sulfonated poly(ether ether ketone) (SPEEK) hybridized with sulfated zirconia-supported platinum (Pt/S−ZrO_2) catalyst for fuel cell applications. The SPEEK/Pt−S−ZrO_2 membrane exhibited higher water uptake and proton conductivity as well as higher single cell performance under dry operation than the plain SPEEK membrane. Moreover, the enhanced open circuit voltage (OCV) up to 1.015 V and the decreased area ohmic resistance further demonstrated that Pt/S−ZrO_2 in the membrane could effectively suppress reactant crossover and improve membrane self-humidification as well.

9.4. Other Oxides

9.4.1. $RuO_2 \cdot xH_2O$. Ruthenium oxide (RuO_2) has also been explored as a catalyst support.[369] The Pt/RuO_2 catalyst shows the bifunctional mechanism in methanol oxidation,[370,371] in which the presence of Ru−OH bonds on the RuO_2 surface plays a beneficial role in catalytic activity enhancement for methanol oxidation. It is believed that $Ru-OH_{ad}$ can facilitate $Pt-CO_{ad}$ oxidation at a lower potential by providing adsorbed OH_{ad} groups adjacent to active Pt atoms. To further exploit this beneficial property of the Pt/RuO_2 catalyst, new strategies for synthesizing novel $RuO_2 \cdot xH_2O$-supported Pt catalyst have been proposed. For example, Chen et al.[372] employed a solution-phase method to synthesize hydrous ruthenium oxide-supported platinum catalyst ($Pt/RuO_2 \cdot xH_2O$). This catalyst showed higher catalytic reactivity toward methanol oxidation than that of E-TEK Pt−Ru black catalyst.

9.4.2. Si-Based Oxides (SiO_2). Recently, SiO_2-supported Pt catalyst was explored in the preparation of self-humidifying membranes in PEM fuel cells. For example, Zhu et al.[366] and Wang[373] developed novel self-humidifying reinforced composite membranes. They found that fuel cell performance could be improved due to the presence of hydrophilic Pt/SiO_2 catalyst. Several beneficial effects when the membrane was

modified by this Pt/SiO_2 material were observed such as membrane resistance reduction,[373] anode self-humidification improvement, cathode polarization reduction, as well as OCV value increase.[369] For this Pt/SiO_2 catalyst, a high catalytic activity toward the oxygen reduction reaction was also observed, which was attributed to the uniform dispersion of Pt on the interconnected particle network of SiO_2, maximizing the available electrochemical active area. Seger et al.[374] demonstrated that Pt/SiO_2 was a better cathode catalyst for PEM fuel cells than was Pt-black catalyst. Unfortunately, the electronic conductivity of SiO_2 is quite low, limiting its practical usage as a catalyst in PEM fuel cells. More effort should be put on how to increase its conductivity using innovative approaches such as doping.

9.4.3. Indium Tin Oxide (ITO, Sn−In_2O_3). Indium tin oxide (ITO) is a degenerated n-type semiconductor with a wide band gap, which is formed by replacing In^{3+} by Sn^{4+} in the cubic bixbyite structure of indium oxide. This replacement produces free electrons enhancing its conductivity and correspondingly influences the optical and electrical properties of the ITO film.[375,376] ITO is a commercially available material often used as a transparent conducting oxide (TCO) for smart windows. Chhina et al.[377] prepared an ITO-supported Pt catalyst as a potential noncarbon catalyst support and studied its thermal and electrochemical stability. The Pt on ITO (38 nm particle size) had an average crystallite sizes of 13 nm. Electrochemical measurements, in which the electrode coated by this Pt/ITO catalyst was cycled between +0.6 and +1.8 V vs SHE for 100 cycles, showed that this catalyst was much more stable than those of both commercially available Hispec 4000 and Pt/Vulcan XC-72R. TGA tests for thermal stability confirmed that the Pt/ITO was stable with only ∼1 wt % loss of ITO material versus ∼57 wt % loss of Hispec 4000 at 1000 °C.

10. CONCLUSIONS

To date, carbon-based supporting materials including various nanostructured carbon materials for Pt-based catalysts have proved to be the most practical catalyst supports for PEM fuel cell catalysts. However, carbon oxidation or corrosion driven by the presence of O_2 and/or high electrode potential has been identified as one of the major failure modes for PEM fuel cell degradation, in particular at higher temperature operation (95−200 °C). To address this issue of carbon oxidation, great effort has been placed in recent years on developing alternative noncarbon materials for catalyst supports. Unfortunately, up to now, there has been no major breakthrough in this area. Under the strong driving force for fuel cell commercialization, the demand to replace carbon supports using other intrinsically stable materials becomes more necessary and urgent.

This review has extensively reviewed the current technical state and the progress in the areas of catalyst support material selection, synthesis and characterization, as well as fuel cell validation. The reviewed noncarbon materials include nitrides, carbides, mesoporous silicas, conducting polymers, and metal oxides. As compared to carbon-based supports, some noncarbon materials and their supported Pt-based catalysts have shown unique structures, suitable physical and chemical properties, and high catalytic activity toward fuel cell reactions such as the oxygen reduction reaction and small alcohol electrooxidation. In terms of catalyst stability, some noncarbon materials have intrinsic inertness to high temperatures and corrosive electrochemical environments, significantly improving the stability of the supports as well as their supported catalysts, leading to high durability for the fuel cell. In comparison with commercially available carbon-supported Pt or Pt alloy catalysts, some noncarbon-supported Pt or Pt alloy catalysts have shown superior performance in both activity and stability and strong poison-tolerance capability. Regarding these activity and stability enhancements, as well as poison-tolerance capability, the synergistic interaction between Pt and noncarbon support has been identified as the major contributor to these beneficial effects. Moreover, the uniform distribution of metal catalyst particles on nanostructured noncarbon supports can also make a contribution to the catalytic enhancement.

In comparison with carbon supports, some significant drawbacks still exist for noncarbon-based supports. First and foremost is the electronic conductivity because it appears that almost all noncarbon materials have lower electronic conductivity when compared to carbon materials. The second drawback is solubility because the majority of noncarbon support materials have higher solubility than carbon materials in aqueous environments, particularly in the acidic environment in which PEM fuel cell reactions occur. The third drawback is electrochemical and chemical stability because some noncarbon support materials, such as WC, are easier to oxidize at oxygen electrode potentials than carbon materials, leading to failure. The fourth drawback is thermal stability because some noncarbon support materials such as conductive polymers are not stable at higher temperatures, that is, >100 °C. Finally, the fifth drawback is low surface area because it seems that almost all noncarbon supports have lower surface area when compared to carbon materials. For an effective fuel cell catalyst, large surface area is often a necessary factor determining the catalyst activity. Therefore, to make noncarbon-supported Pt-based catalysts practically feasible in PEM fuel cells, material improvements in electronic conductivity, solubility, chemical/electrochemical and thermal stability, and surface area are required. Materials trade-offs will likely be required for noncarbon catalyst supports because it will be very difficult to meet all of the required materials improvements. To meet some of these material requirements, the following research areas can be proposed:

(1) Developing novel synthesis methods to modify and create new support materials, which have improved electronic conductivity, insolubility, electrochemical and thermal stabilities, as well as high surface area. For example, material doping strategies have been proved to be an effective way to improve conductivity, solubility, and electrochemical and thermal stabilities. Modifying the composition of support materials such as the ratio of components can also improve the material's properties and make them feasible catalyst supports. Regarding support surface area improvement, synthesis of nanostructured material particles such as nanotubes, nanospheres, nanorods, nanofibers, and nanohiearchial structures should be an effective way to achieve high surface areas and improve the catalytic activity.

(2) Developing catalyst deposition strategies to make a uniform dispersion of Pt or Pt alloy particles on the support, and a strong synergistic interaction between the catalyst and support particles. This strategy could produce positive electronic and chemical interactions between the catalyst particle and the support. Interaction enhancement of metals like Pt or Pt alloy catalysts with noncarbon supports through various experimental approaches would be an interesting research area in the

effort to improve both the stability and the activity of noncarbon-supported Pt-based catalysts in PEM fuel cell applications. The research objectives would be (a) improving the electronic conductivity of the support, (b) increasing the surface area of the support, (c) enhancing the physicochemical stability of the support, and (d) developing catalysts with a highly uniform distribution of Pt or Pt alloy.

(3) Establishing a fundamental understanding of the noncarbon support through both experimental and modeling approaches, for example, exploration of morphology effects of noncarbon-supported catalyst on both the catalytic activity and the stability, as well as the interaction between the catalyst and support particles for the oxygen reduction reaction. Theoretical modeling such as quantum chemical calculation should provide some guidance for the down-selection of new supports and their supported catalyst designs.

(4) Optimizing fuel cell design and operation to avoid the catalyst drawbacks and promote the advantages of the catalyst material. As mentioned previously, it will be extremely difficult to have a catalyst material that can meet all requirements.

It is unlikely that any support system will be able to address all requirements (high electronic conductivity, low solubility, high chemical/electrochemical and thermal stability, and high surface area) at the same time. Some trade-offs may be reasonable in solving this support material problem. We believe that the trade-offs are strongly dependent on the individual materials and their supported catalysts as well as fuel cell application requirements. However, to realize the real commercialization of PEM fuel cells, current technological gaps must be closed, and a suitable electrocatalyst for oxygen reduction is a key goal. Noncarbon supports for Pt-based electrocatalysts seem to be an effective and necessary way (may be the only way) to eliminate carbon support corrosion and oxidation during PEM fuel cell operation, particularly at high temperatures (95−200 °C). It is clear that a more intensive research effort should be put on the development of noncarbon-supported catalysts.

AUTHOR INFORMATION

Corresponding Author

*Tel.: (604) 822-4888 (D.P.W.); (604) 221-3087 (J.Z.). E-mail: dwilkinson@chbe.ubc.ca (D.P.W.); jiujun.zhang@nrc.gc.ca (J.Z.).

BIOGRAPHIES

Dr. Yan-Jie Wang obtained his M.S. in Materials from North University of China in 2002. He then studied his Ph.D. program under the supervision of Dr. Yi Pan in Zhejiang University and was awarded a Ph.D. Degree in Materials Science and Engineering in March 2005. After two and half postdoctoral years spent in Sungkyunkwan University in Korea on Advanced Functional Materials, he worked on Materials in Prof. Ralph H. Colby's group as a postdoctoral scholar at the Pennsylvania State University. In 2009, he joined Dr. David P. Wilkinson's group as a postdoctoral researcher at the University of British Columbia. Currently, he is working on fuel cell catalysts under the supervision of Dr. David P. Wilkinson and Dr. Jiujun Zhang at the National Research Council of Canada Institute for Fuel Cell Innovation (NRC-IFCI).

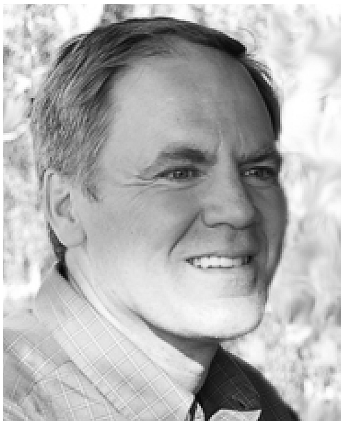

Dr. David P. Wilkinson received his B.A.Sc. degree in Chemical Engineering from the University of British Columbia (UBC) in 1978 and his Ph.D. degree in Chemistry from the University of Ottawa in 1987 where his graduate work was done with Dr. Brian Conway. He has over 20 years of industrial experience in the areas of fuel cells and advanced rechargeable lithium batteries. In 2004, Dr. Wilkinson was awarded a Tier 1 Canada Research Chair in Clean Energy and Fuel Cells in the Department of Chemical and Biological Engineering at the University of British Columbia. He is currently the Director of the Clean Energy Research Centre (CERC) at the university. He maintains a joint appointment with the University and the Canadian National Research Council Institute for Fuel Cell Innovation. Prior to his university appointment, Dr. Wilkinson was the Director and then Vice President of Research and Development at Ballard Power Systems Inc., involved with the research, development, and application of fuel cell technology. Dr. Wilkinson is one of the leading all-time fuel cell inventors by issued U.S. patents. Dr. Wilkinson's main research interest is in electrochemical power sources and processes to create clean and sustainable energy.

Dr. Jiujun Zhang received his B.Sc and M.Sc from Peking University in 1982 and 1985, and his Ph.D. in Electrochemistry from Wuhan University in 1988, and he is now a Senior Research Officer and PEM Catalysis Core Competency Leader at the National Research Council of Canada Institute for Fuel Cell Innovation (NRC-IFCI). Dr. Zhang holds several adjunct professorships, including one at the University of Waterloo and one at the University of British Columbia. His research is mainly based on fuel cell catalysis development.

ACKNOWLEDGMENT

We would like to thank the National Research Council of Canada Institute for Fuel Cell Innovation (NRC-IFCI) and the NRC/NRCan/NSERC Hydrogen and Fuel Cell Program for their financial support. We would also like to acknowledge the contribution from Dr. Hui Li and all members of the NRC catalyst groups.

REFERENCES

(1) Giddey, S.; Ciacchi, F. T.; Badwal, S. P. S.; Zelizko, V.; Edwards, J. H.; Duffy, G. J. *Solid State Ionics* **2000**, *152*, 363.
(2) Herring, A. M.; Zawodzinski, T. A., Jr.; Hamrock, S. J. *Fuel Cell Chemistry and Operation*; ACS Symposium Series; American Chemical Society: Washington, DC, 2010.
(3) Vogel, J. U.S. DOE Hydrogen Program 2008 Annual Progress Report. http://www.hydrogen.energy.gov/pdfs/progress08/v_d_4_vogel.pdf.
(4) Hydrogen, Fuel Cells & Infrastructure Technologies Program, Multi-Year Research, Development and Demonstration Plan, October 2007, Table 3.4.2.
(5) Hoogers, G. *Fuel Cell Technology Handbook*; CRC Press: Boca Raton, London, New York, Washington, DC, 2003.
(6) Ahmed, K.; Föger, K. *Ind. Eng. Chem. Res.* **2010**, *49*, 7239.
(7) Verhelst, S.; Wallner, T. *Prog. Energy Combust.* **2009**, *35*, 490.
(8) Thomas, C. E. *Int. J. Hydrogen Energy* **2009**, *34*, 6005.
(9) Appleby, A. J.; Dudley, R.; Grady, W. O.; Srinivasan, S. *Electrochem. Soc. Proc. Ser.* **1979**, *79-2*, 23.
(10) Mathias, M.; Makharia, R.; Gasteiger, H.; Conley, J.; Fuller, T.; Gittleman, C.; Kocha, S.; Miller, D.; Mittesteadt, C.; Xie, T.; Yan, S.; Yu, P. *Interface* **2005**, *14*, 24.
(11) Franco, A. A.; Guinard, M.; Barthe, B.; Lemaire, O. *Electrochim. Acta* **2009**, *54*, 5267.
(12) Cameron, D. S. *Platinum Met. Rev.* **2009**, *53*, 147.
(13) Yu, P. T.; Gu, W.; Zhang, J.; Makharia, R.; Wagner, F. T.; Gasteiger, H. A. *Polymer Electrolyte Fuel Cell Durability*; Springer: New York, 2009.
(14) Lim, D.-H.; Lee, W.-J.; Wheldon, J.; Macy, N. L.; Smyrl, W. H. *J. Electrochem. Soc.* **2010**, *157*, B862.
(15) Adzic, R. R.; Zhang, J.; Sasaki, K.; Vukmirovic, M. B.; Shao, M.; Wang, J. X.; Nilekar, A. U.; Mavrikakis, M.; Valerio, J. A.; Uribe, F. *Top. Catal.* **2007**, *46*, 249.
(16) Lee, K.; Zhang, J.; Wang, H.; Wilkinson, D. P. *J. Appl. Electrochem.* **2006**, *36*, 507.
(17) Serp, P.; Corrias, M.; Kalck, P. *Appl. Catal., A* **2003**, *253*, 337.
(18) Antolini, E. *Appl. Catal., B* **2009**, *88*, 1.
(19) Schmidt, T. J.; Gasteiger, H. A.; Stab, G. D.; Urban, P. M.; Kolb, D. M.; Behm, R. J. *J. Electrochem. Soc.* **1998**, *145*, 2354.
(20) Passalacqua, E.; Lufrano, F.; Squadrito, G.; Patti, A.; Giorgi, L. *Electrochim. Acta* **2001**, *46*, 799.
(21) Min, M.; Cho, J.; Cho, K.; Kim, H. *Electrochim. Acta* **2000**, *45*, 4211.
(22) Shao, Y. Y.; Yin, G. P.; Gao, Y. Z. *J. Power Sources* **2007**, *171*, 558.
(23) Stevens, D. A.; Hicks, M. T.; Haugen, G. M.; Dahn, J. R. *J. Electrochem. Soc.* **2005**, *152*, A2309.
(24) Shao, Y.; Liu, J.; Wang, Y.; Lin, Y. *J. Mater. Chem.* **2009**, *19*, 46.
(25) Knights, S. D.; Colbow, K. M.; St-Pierre, J.; Wilkinson, D. P. *J. Power Sources* **2004**, *127*, 127.
(26) Zhang, S.; Yuan, X.; Wnag, H.; Mérida, W.; Zhu, H.; Shen, J.; Wu, S.; Zhang, J. *Int. J. Hydrogen Energy* **2009**, *34*, 388.
(27) Li, H.; Song, C.; Hui, R.; Zhang, J.; Zhang, J. In *PEM Fuel Cell Electrocatalysts and Catalyst Layers: Fundamentals and Applications*; Zhang, J., Ed.; Springer: New York, 2008.
(28) Shao, Y.; Liu, J.; Wang, Y.; Lin, Y. *J. Mater. Chem.* **2009**, *19*, 46.
(29) Zhou, J. G.; Zhou, X. T.; Sun, X. H.; Li, R. Y.; Murphy, M.; Ding, Z. F.; Sun, X. L.; Sham, T. K. *Chem. Phys. Lett.* **2007**, *437*, 229.
(30) Attard, G. A.; Bannister, A. *J. Electroanal. Chem.* **1991**, *300*, 467.
(31) Greeley, J.; Nørskov, J. K.; Mavrikakis, M. *Annu. Rev. Phys. Chem.* **2002**, *53*, 319.
(32) Rodriguez, J. A. *Surf. Sci. Rep.* **1996**, *24*, 225.
(33) Seger, B.; Kongkanand, A.; Vinodgopal, K.; Kamat, P. V. *J. Electroanal. Chem.* **2008**, *621*, 198.
(34) Setthapun, W.; Bej, S. K.; Thompson, L. T. *Top. Catal.* **2008**, *49*, 73.
(35) Cote, R.; Lalande, G.; Faubert, G.; Guay, D.; Dodelet, J. P.; Denes, G. *J. New Mater. Electrochem. Syst.* **1998**, *1*, 7.
(36) Eswaramoorthi, I.; Dalai, A. K. *Int. J. Hydrogen Energy* **2009**, *34*, 2580.
(37) Kónya, Z.; Puntes, V. F.; Kiricsi, I.; Zhu, J.; Ager, J. W.; Ko, M. K.; Frei, H.; Alivisatos, P.; Somorjai, G. A. *Chem. Mater.* **2003**, *15*, 1242.
(38) Laborde, H.; Leger, J.-M.; Lamy, C. *J. Appl. Electrochem.* **1994**, *24*, 1019.
(39) Bouzek, K.; Mangold, K.-M.; Jüttner, K. *Electrochim. Acta* **2000**, *46*, 661.
(40) Prakash, J.; Tryk, D. A.; Aldred, W.; Yeager, E. B. *J. Appl. Electrochem.* **1999**, *29*, 1463.
(41) Bacon, F. T. In *Fuel Cells*; Young, G. J., Ed.; Reinhold Publishing Co.: New York, 1960; Vol. I.
(42) Landi, H. P.; Voorhies, J. D.; Barber, W. A. In *Fuel Cell Systems II*; Gould, R. F., Ed.; American Chemical Society: Washington, DC, 1969.
(43) Chan, K.-Y.; Ding, J.; Ren, J.; Cheng, S.; Tsang, K. Y. *J. Mater. Chem.* **2004**, *14*, 505.
(44) Yu, X.; Ye, S. *J. Power Sources* **2007**, *172*, 133.
(45) Zhang, J.; Tang, Y.; Song, C.; Zhang, J. *J. Power Sources* **2007**, *172*, 163.
(46) Song, C.; Tang, Y.; Zhang, J.; Zhang, J.; Wang, H.; Shen, J.; McDermid, S.; Li, J.; Kozak, P. *Electrochim. Acta* **2007**, *51*, 2552.
(47) Wu, J.; Yuan, X. Z.; Martin, J. J.; Wang, H.; Zhang, J.; Shen, J.; Wu, S.; Merida, W. *J. Power Sources* **2008**, *184*, 104.
(48) Virkar, A. V.; Zhou, Y. *J. Electrochem. Soc.* **2007**, *154*, B540.
(49) Passalacqua, E.; Vivaldi, M.; Giordano, N.; Anotonucci, P. L.; Kinoshita, K. *Proceedings of the 27th Intersociety Energy Conversion Engineering Conf.*; 1992; Vol. *929294*, pp 3.425−3.431.
(50) Billings, R. E. *The Hydrogen World View*; American Academy of Science, 1991.
(51) Garland, N. Fuel Cells Plenary; 2008 DOE Hydrogen Program Merit Review and Peer Evaluation Meeting, 2008.
(52) Shim, J.; Lee, C.-R.; Lee, H.-K.; Lee, J.-S.; Cairns, E. J. *J. Power Sources* **2001**, *102*, 172.
(53) Xiong, L.; Manthiram, A. *Electrochim. Acta* **2004**, *49*, 4163.
(54) Chen, J.; Sarma, L. S.; Chen, C.; Cheng, M.; Shih, S.; Wang, G.; Liu, D.; Lee, J.; Tang, M.; Hwang, B. *J. Power Sources* **2006**, *159*, 29.
(55) Janik, M. J.; Taylor, C. D.; Neurock, M. *J. Electrochem. Soc.* **2009**, *156*, B126.
(56) Neurock, M.; Janik, M. J.; Wasileski, S. A.; Anderson, A.; Mukerjee, S. *AIChE Annual Meeting* **2005**, 510d.
(57) Nørskov, J. K.; Bligaard, T.; Hvolbæk, B.; bild-Pedersen, F.; Chorkendorff, I.; Christensen, C. H. *Chem. Soc. Rev.* **2008**, *37*, 2163.
(58) Stamenkovic, V.; Mun, B. S.; Mayrhofer, K. J. J.; Ross, P. N.; Markovic, N. M.; Rossmeisl, J.; Greeley, J.; Nørskov, J. K. *Angew. Chem., Int. Ed.* **2006**, *45*, 2897.
(59) Fialkov, A. S. *Russ. J. Electrochem.* **2000**, *36*, 389.

(60) Fialkov, A. S.; Leclerc, C.; Contour, J. P. *Catalysis* **1973**, *29*, 31.
(61) Hillenbrand, L. J.; Lacksonen, J. W. *J. Electrochem. Soc.* **1965**, *112*, 249.
(62) Coloma, F.; Sepulveda, A.; Fierro, J.; Rodriguez-Reinoso, F. *Appl. Catal., A* **1996**, *148*, 63.
(63) Shukla, A. K.; Ravikumar, M. K.; Roy, A.; Barman, S. R.; Sarma, D. D.; Aricò, A. S.; Antonucci, V.; Pino, L.; Giordano, N. *J. Electrochem. Soc.* **1994**, *141*, 1517.
(64) Shukla, A.; Ramesh, K.; Manoharan, R.; Sarode, P.; Vasudevan, S. *Ber. Bunsen-Ges. Phys. Chem.* **1985**, *89*, 1261.
(65) Antolini, E.; Giorgi, L.; Cardellini, F.; Passalacqua, E. *J. Solid State Electrochem.* **2001**, *5*, 131.
(66) Goodenough, J. B.; Manoharan, R. *Chem. Mater.* **1989**, *1*, 391.
(67) McBreen, J.; Mukerjee, S. *J. Electrochem. Soc.* **1995**, *142*, 3399.
(68) Kim, T.; Kobayashi, K.; Nagain, M. *J. Oleo Sci.* **2007**, *50*, 553.
(69) Vedrine, J. C.; Dufaux, M.; Naccache, C.; Imelik, B. *J. Chem. Soc., Faraday Trans.* **1978**, *74*, 440.
(70) Biloul, A.; Coowar, F.; Contamin, O.; Scarbeck, G.; Savy, M.; Van den Ham, D.; Riga, J.; Verbist, J. *J. Electroanal. Chem.* **1990**, *289*, 189.
(71) Bogotski, V. S.; Snudkin, A. M. *Electrochim. Acta* **1984**, *29*, 757.
(72) Kobelev, A. V.; Kobeleva, R. M.; Ukhov, V. F. *Dokl. Akad. Nauk USSR* **1978**, *243*, 692.
(73) De Miguel, S.; Scelza, O.; Romanmartinez, M.; Salinas-Martinez, C.; Cazorlaamoros, D.; Linares-Solano, A. *Appl. Catal., A* **1998**, *170*, 93.
(74) Van dam, H.; Van Bekkum, H. *J. Catal.* **1991**, *131*, 335.
(75) Czaran, E.; Finster, J.; Schnabel, K. *Z. Anorg. Allg. Chem.* **1978**, *443*, 175.
(76) Lopez-Ramon, M.; Stoekli, F.; Morenocastilla, C.; Carrasco-Marin, F. *Carbon* **1999**, *37*, 1215.
(77) Barton, S.; Evans, M.; Halliop, E.; Macdonald, J. *Carbon* **1997**, *35*, 1361.
(78) Leon, C.; Leon, Y.; Solar, J.; Calemma, V.; Radovic, L. *Carbon* **1992**, *30*, 797.
(79) Lambert, J.; Che, M. *J. Mol. Catal. A* **2000**, *162*, 5.
(80) Petrii, O. A.; Kazarinov, V. E. *Elektrokhimiya* **1965**, *1*, 1389.
(81) Petrii, O. A. *Dokl. Akad. Nauk SSSR* **1965**, *160*, 871.
(82) Entina, V. S.; Petrii, O. A. *Elektrokhimiya* **1968**, *4*, 678.
(83) Chen, G.; Xia, D. G.; Nie, Z. R.; Wang, Z. Y.; Wang, L.; Zhang, L.; Zhang, J. *J. Chem. Mater.* **2007**, *19*, 1840.
(84) Kinoshita, K.; Bett, J. A. S. *Carbon* **1975**, *11*, 403.
(85) Tian, Z. Q.; Jiang, S. P.; Liang, Y. M.; Shen, P. K. *J. Phys. Chem. B* **2006**, *110*, 5343.
(86) Binder, H.; Kbhling, A.; Sandstede, G. In *From Electrocatalysis to Fuel Cells*; Sandstede, G., Ed.; University of Washington Press: Seattle, WA, 1972; pp 43−58.
(87) McNicol, B. D.; Short, R. T. *J. Electroanal. Chem.* **1977**, *81*, 249.
(88) Friedrich, K. A.; Geyzers, K.-P.; Linke, U.; Stimming, U.; Stumper, J. *J. Electroanal. Chem.* **1996**, *402*, 123.
(89) Frelink, T.; Visscher, W.; Van Veen, J. A. R. *Langmuir* **1996**, *12*, 3702.
(90) Chrzanowski, W.; Wieckowski, A. *Langmuir* **1997**, *13*, 5974.
(91) Brankovic, S. R.; McBreen, J.; Adzic, R. R. *J. Electroanal. Chem.* **2001**, *503*, 99.
(92) Brankovic, S. R.; Wang, J. X.; Adzic, R. R. *Electrochem. Solid-State Lett.* **2001**, *4*, A217.
(93) Sasaki, K.; Mo, Y.; Wang, J. X.; Balasubramanian, M.; Uribe, F.; McBreen, J.; Adzic, R. R. *Electrochim. Acta* **2003**, *48*, 3841.
(94) Zhang, J.; Mo, Y.; Vukmirovic, M. B.; Klie, R.; Sasaki, K.; Adzic, R. R. *J. Phys. Chem. B* **2004**, *108*, 10955.
(95) Stamenkovic, V.; Schmidt, T. J.; Ross, P. N.; Markovic, N. M. *J. Phys. Chem. B* **2002**, *106*, 11970.
(96) Stamenkovic, V.; Schmidt, T. J.; Ross, P. N.; Markovic, N. M. *J. Electroanal. Chem.* **2003**, *554*, 191.
(97) Stamenkovic, V. R.; Mun, B. S.; Mayrhofer, K. J. J.; Ross, P. N.; Markovic, N. M. *J. Am. Chem. Soc.* **2006**, *128*, 8813.
(98) Stamenkovic, V. R.; Mun, B. S.; Arenz, M.; Mayrhofer, K. J. J.; Lucas, C. A.; Wang, G.; Ross, P. N.; Markovic, N. M. *Nat. Mater.* **2007**, *6*, 241.
(99) Stamenkovic, V. R.; Fowler, B.; Mun, B. S.; Wang, G.; Ross, P. N.; Lucas, C. A.; Markovic, N. M. *Science* **2007**, *315*, 493.
(100) Zhang, J.; Vukmirovic, M. B.; Xu, Y.; Mavrikakis, M.; Adzic, R. R. *Angew. Chem., Int. Ed.* **2005**, *44*, 2132.
(101) Zhang, J.; Vukmirovic, M. B.; Sasaki, K.; Nilekar, A. U.; Mavrikakis, M.; Adzic, R. R. *J. Am. Chem. Soc.* **2005**, *127*, 12480.
(102) Naohara, H.; Ye, S.; Uosaki, K. *Electrochim. Acta* **2000**, *45*, 3305.
(103) Brankovic, S. R.; McBreen, J.; Adzic, R. R. *Surf. Sci.* **2001**, *479*, L363.
(104) Brankovic, S. R.; Wang, J. X.; Adzic, R. R. *Surf. Sci.* **2001**, *477*, L173.
(105) Levy, R. B.; Boudart, M. *Science* **1973**, *181*, 547.
(106) Dhandapani, B.; Clair, T. S.; Oyama, S. T. *Appl. Catal., A* **1998**, *168*, 219.
(107) Furimsky, E. *Appl. Catal., A* **2003**, *240*, 1.
(108) Mazza, F.; Trassatti, S. *J. Electrochem. Soc.* **1963**, *110*, 847.
(109) Datta, M.; Kumta, P. 212th Meeting Electrochemical Society, 2007, Abstract 10.
(110) Evans, S. A. G.; Terry, J. G.; Plank, N.; Walton, A.; Keane, L.; Campbell, C.; Ghazal, P.; Beattie, J.; Su, T.; Crain, J.; Mount, A. *Electrochem. Commun.* **2005**, *7*, 125.
(111) Wang, Y.; Yuan, H.; Lu, X.; Zhou, Z.; Xiao, D. *Electroanalysis* **2006**, *18*, 15.
(112) Cesiulis, H.; Ziomek-Moroz, M. *J. Appl. Electrochem.* **2000**, *30*, 1261.
(113) Nakayama, T.; Wake, H.; Ozawa, K.; Kodama, H.; Nakamura, N.; Matsunaga, T. *Environ. Sci. Technol.* **1998**, *32*, 798.
(114) Musthafa, O. T.; Sampath, S. *Chem. Commun.* **2008**, 67.
(115) Giner, J.; Swette, L. *Nature* **1966**, *211*, 1291.
(116) Merzougui, B.; Halalay, I. C.; Carpenter, M. K.; Swathirajan, S. U.S. Patent 20060251954 A1, 2006.
(117) Oyama, S. T. *The Chemistry of Transition Metal Carbides and Nitrides*; Springer: London, 1996.
(118) Avasarala, B.; Murray, T.; Li, W.; Haldar, P. *J. Mater. Chem.* **2009**, *19*, 1803.
(119) Avasarala, B.; Haldar, P. *Electrochim. Acta* **2010**, doi:10.1016/j.electacta.2010.08.035
(120) Wells, A. F. *Structural Inorganic Chemistry*, 5th ed.; Clarendon Press: Oxford, 1984.
(121) Paine, R. T.; Nitride, C. K. *Chem. Rev.* **1990**, *90*, 73.
(122) Wu, J. C.; Lin, Z.; Pan, F. J. W.; Rei, M. *Appl. Catal., A* **2001**, *219*, 117.
(123) Lin, C. A.; Wu, J. C. S.; Pan, F. J. W.; Yeh, C. T. *J. Catal.* **2002**, *210*, 39.
(124) Sumiya, H.; Sato, S.; Yazu, S. U.S. Patent 5,332,629, 1994.
(125) Perdigon-Melon, J. A.; Auroux, A.; Guimon, C.; Bonnetot, B. *J. Solid State Chem.* **2004**, *177*, 609.
(126) Patt, J. J.; Moon, D. J.; Phillips, C.; Thompson, L. T. *Catal. Lett.* **2000**, *65*, 193.
(127) Patt, J. J.; Bej, S. K.; Thompson, L. T. *Stud. Surf. Sci. Catal.* **2004**, *147*, 85.
(128) Bej, S. K.; Ranganathan, E. S.; Thompson, L. T. *Abstr. Pap. Am. Chem. Soc.* **2003**, *225*, U867.
(129) Patt, J. J. Carbide and nitride catalysts for the water gas shift reaction. Ph.D. Dissertation, University of Michigan, 2003.
(130) Thompson, L. T.; Bej, S. K.; Patt, J. J.; Kim, C. H. U.S. Patent 6,897,178 B1, 2005.
(131) Antolini, E.; Gonzalez, E. R. *Solid State Ionics* **2009**, *180*, 746.
(132) Hwu, H. H.; Chen, J. G. *Chem. Rev.* **2005**, *105*, 185.
(133) Oyama, S. T. *Catal. Today* **1992**, *15*, 179.
(134) Grubb, W. T.; McKee, D. W. *Nature* **1966**, *210*, 192.
(135) White, E. R.; Maget, H. J. R. *Proc. 19th Ann. Power Sources Conf.* **1965**, 46.
(136) McKee, D. W.; Scarpellino, A. J.; Danzig, I. F.; Pak, M. S. *J. Electrochem. Soc.* **1969**, *116*, 562.
(137) Suggs, A. M.; Dean, R. S. U.S. Patent 2,636,856, 1953.
(138) Jalan, V.; Frost, D. G. U.S. Patent 4,795,684, 1989.

(139) Sung, I.-K.; Mitchell, C. M.; Kim, D.-P.; Kenis, P. J. A. *Adv. Funct. Mater.* **2005**, *15*, 1336.
(140) Schwetz, K. A. In *Handbook of Ceramic Hard Materials*; Riedel, R., Ed.; Wiley-VCH: Weinheim, 2000; Vol. 1, pp 683−740.
(141) Ledoux, M. J.; Pham-Huu, C. *CATTECH* **2001**, *5*, 226.
(142) Honji, A.; Mori, T.; Hishinuma, Y. *J. Electrochem. Soc.* **1988**, *135*, 917.
(143) Venkateswara Rao, Ch.; Singh, S. K.; Viswanathan, B. *Indian J. Chem.* **2008**, *47A*, 1619.
(144) Jalan, V.; Taylor, E. T.; Frost, D.; Morriseau, B. *National Fuel Cell Semin. Abstr.* **1983**, 127.
(145) Krawiec, P.; Kaskel, S. *J. Solid State Chem.* **2006**, *179*, 2281.
(146) Ledoux, M. J.; Hantzer, S.; Huu, C. P.; Guille, J.; Desaneaux, M. P. *J. Catal.* **1988**, *114*, 176.
(147) Jin, G. Q.; Guo, X. Y. *Microporous Mesoporous Mater.* **2003**, *60*, 207.
(148) Parmentier, J.; Patarin, J.; Dentzer, J.; Vix-Guterl, C. *Ceram. Int.* **2002**, *28*, 1.
(149) Liu, Z. C.; Shen, W. H.; Bu, W. B.; Chen, H. R.; Hua, Z. L.; Zhang, L. X.; Li, L.; Shi, J. L.; Tan, S. H. *Microporous Mesoporous Mater.* **2005**, *82*, 137.
(150) Lu, A. H.; Schmidt, W.; Kiefer, W.; Schuth, F. *J. Mater. Sci.* **2005**, *40*, 5091.
(151) Pol, V. G.; Pol, S. V.; Gedanken, A. *Chem. Mater.* **2005**, *17*, 1797.
(152) Bohm, H. *Nature* **1970**, *227*, 483.
(153) Hwu, H. H.; Chen, J. G.; Kourtakis, K.; Lavin, J. G. *J. Phys. Chem. B* **2001**, *105*, 10037.
(154) Zellner, M. B.; Chen, J. G. *J. Electrochem. Soc.* **2005**, *152*, A1483.
(155) Barnett, C. J.; Burstein, G. T.; Kucernak, A. R. J.; Williams, K. R. *Electrochim. Acta* **1997**, *42*, 2381.
(156) McIntyre, D. R.; Burstein, G. T.; Vossen, A. *J. Power Sources* **2002**, *107*, 67.
(157) Ganesan, R.; Lee, J. S. *Angew. Chem., Int. Ed.* **2005**, *44*, 6557.
(158) Venkataraman, R.; Kunz, H. R.; Fenton, J. M. *J. Electrochem. Soc.* **2003**, *150*, A278.
(159) Yang, X. G.; Wang, C. Y. *Appl. Phys. Lett.* **2005**, *86*, 224104.
(160) Zoltowski, P. *Electrochim. Acta* **1986**, *31*, 103.
(161) Lee, K.; Ishihara, A.; Mitsushima, S.; Kamiya, N.; Ota, K.-I. *Electrochim. Acta* **2004**, *49*, 3479.
(162) Ribeiro, F. H.; Dalla Betta, R. A.; Guskey, G. J.; Boudart, M. *Chem. Mater.* **1991**, *3*, 805.
(163) Katrib, A.; Hemming, F.; Wehrer, P.; Hilaire, L.; Maire, G. *Top. Catal.* **1994**, *1*, 75.
(164) Liang, C.; Ding, L.; Wang, A.; Ma, Z.; Qiu, J.; Zhang, T. *Ind. Eng. Chem. Res.* **1009**, *48*, 3244.
(165) Shanmugam, S.; Jacob, D. S.; Gedanken., A. *J. Phys. Chem. B* **2005**, *109*, 19056.
(166) Chhina, H.; Campbell, S.; Kesler, O. *J. Power Sources* **2007**, *164*, 431.
(167) Hwu, H. H.; Chen, J. G. G. *J. Vac. Sci. Technol., A* **2003**, *21*, 1488.
(168) Cottrell, A. H. *Chemical Bonding in Transition Metal Carbides*; The Institute of Materials: London, 1995; p 77.
(169) Gao, L.; Kear, B. H. *Nanostruct. Mater.* **1995**, *5*, 555.
(170) Hatano, Y.; Takamori, M.; Matsuda, K.; Ikeno, S.; Fujii, K.; Watanabe, K. *J. Nucl. Mater.* **2002**, *307−311*, 1339.
(171) Liu, N.; Kourtakis, K.; Figueroa, J. C.; Chen, J. G. *J. Catal.* **2003**, *215*, 254.
(172) Zellner, M. B.; Chen, J. G. *Catal. Today* **2005**, *99*, 299.
(173) Jeon, M. K.; Daimon, H.; Lee, K. R.; Nakahara, A.; Woo, S. I. *Electrochem. Commun.* **2007**, *9*, 2692.
(174) Ganesan, R.; Ham, D. J.; Lee, J. S. *Electrochem. Commun.* **2007**, *9*, 2576.
(175) Hara, Y.; Minami, N.; Itagaki, H. *Appl. Catal., A* **2007**, *323*, 86.
(176) Hara, Y.; Minami, N.; Matsumoto, H.; Itagaki, H. *Appl. Catal., A* **2007**, *332*, 289.
(177) Ham, D. J.; Kim, Y. K.; Han, S. H.; Lee, J. S. *Catal. Today* **2008**, *132*, 117.
(178) Zhang, S.; Zhu, H.; Yu, H.; Hou, J.; Yi, B.; Ming, P. *Chin. J. Catal.* **2007**, *28*, 109.
(179) Cahn, R. W.; Haasen, P.; Kramer, E. J. *Materials Science and Technology*; Swain VCH: Weinheim, 1994; Vol. 11, p 175.
(180) Goor, G. V. D.; Sägesser, P.; Berroth, K. *Solid State Ionics* **1997**, *101−103*, 1163.
(181) Cooper, A. S.; Corenzwit, E.; Longinotti, L. D.; Matthias, B. T.; Zachariasen, W. H. *Proc. Natl. Acad. Sci. U.S.A.* **1970**, *67*, 313.
(182) Yin, S.; Mu, S.; Lv, H.; Cheng, N.; Pan, M.; Fu, Z. *Appl. Catal., B* **2010**, *93*, 233.
(183) Zhang, J. Y.; Fu, Z. Y.; Wang, W. M. *J. Mater. Sci. Technol.* **2005**, *21*, 841.
(184) Basu, B.; Raju, G. B.; Suri, A. K. *Int. Mater. Rev.* **2006**, *51*, 352.
(185) Feng, Y.; Yao, R.; Zhang, L. *Physica B* **2004**, *350*, 348.
(186) Rajesh, K.; Ahuja, T.; Kumar, D. *Sens. Actuators, B* **2009**, *136*, 275.
(187) Skotheim, T. A. *Handbook of Conducting Polymers*; Marcel Dekker: New York, 1986.
(188) Huang, W. S.; Humphrey, B. D.; MacDiarmid, A. G. *J. Chem. Soc., Faraday Trans.* **1986**, *152*, 2385.
(189) Stilwell, D. E.; Park, S. M. *J. Electrochem. Soc.* **1988**, *135*, 2254.
(190) Stilwell, D. E.; Park, S.-M. *J. Electrochem. Soc.* **1988**, *135*, 2491.
(191) Stilwell, D. E.; Park, S.-M. *J. Electrochem. Soc.* **1988**, *135*, 2497.
(192) Stilwell, D. E.; Park, S.-M. *J. Electrochem. Soc.* **1989**, *136*, 427.
(193) Stilwell, D. E.; Park, S.-M. *J. Electrochem. Soc.* **1989**, *136*, 688.
(194) Grnies, E. M.; Boyle, A.; Lapkowski, M.; Tsintavis, C. *Synth. Met.* **1990**, *36*, 139.
(195) Vork, F. T. A.; Janssen, L. J. J.; Barendrecht, E. *Electrochim. Acta* **1986**, *31*, 1569.
(196) Gholamian, M.; Contractor, A. Q. *J. Electroanal. Chem.* **1990**, *289*, 69.
(197) Gholamian, M.; Sundaram, J.; Contractor, A. Q. *Langmuir* **1987**, *3*, 741.
(198) Swathirajan, S.; Mikhail, Y. M. *J. Electrochem. Soc.* **1992**, *139*, 2105.
(199) Strike, D. J.; De Rooij, N. F.; Koudelka-Hep, M.; Ulmann, M.; Augustynski, J. *J. Appl. Electrochem.* **1992**, *22*, 922.
(200) Ulmann, M.; Kostecki, R.; Augustynski, J.; Strike, D. J.; Koudelka-Hep, M. *Chimia* **1992**, *46*, 138.
(201) Kost, K. M.; Bartak, D. E.; Kazee, B.; Kuwana, T. *Anal. Chem.* **1988**, *60*, 2379.
(202) Ocon Esteban, P.; Leger, J.-M.; Lamy, C.; Grnies, E. *J. Appl. Electrochem.* **1989**, *19*, 462.
(203) Laborde, H.; Leger, J.-M.; Lamy, C.; Garnier, F.; Yassar, A. *J. Appl. Electrochem.* **1990**, *20*, 524.
(204) Laborde, H.; Leger, J.-M.; Lamy, C. *J. Appl. Electrochem.* **1994**, *24*, 219.
(205) MacDiarmid, A. G.; Chiang, J. C.; Halpern, M.; Huang, W. S.; Wu, S. L.; Somasiri, N. L. D.; Wu, W.; Yangier, S. I. *Mol. Cryst. Liq. Cryst.* **1985**, *121*, 173.
(206) MacDiarmid, A. G.; Chiang, J. C.; Huang, W.; Humphrey, B. D.; Somasiri, N. L. D. *Mol. Cryst. Liq. Cryst.* **1985**, *125*, 309.
(207) Kim, D. K.; Oh, K. W.; Kim, S. H. *J. Polym. Sci., Part B: Polym. Phys.* **2008**, *46*, 2255.
(208) Li, Z. F.; Ruckenstein, E. *J. Colloid Interface Sci.* **2002**, *251*, 343.
(209) Karir, T.; Hassan, P. A.; Kulshreshtha, S. K.; Samuel, G.; Sivaprasad, N.; Meera, V. *Anal. Chem.* **2006**, *78*, 3577.
(210) MacDiarmid, A. G.; Epstein, A. J. *Synth. Met.* **1995**, *69*, 85.
(211) Chartier, P.; Mattes, B.; Reiss, H. *J. Phys. Chem.* **1992**, *96*, 3556.
(212) Mattoso, L. H. C. *Quim. Nova* **1996**, *19*, 388.
(213) http://www.azom.com/details.asp?ArticleID=1197.
(214) Lamy, C.; Leger, J.-M.; Garnier, F. In *Handbook of Organic Conductive Molecules and Polymers: Conductive Polymers: Spectroscopy and Physical Properties*; Nalwa, H. S., Ed.; John Wiley and Sons: New York, 1997; p 471.

(215) Parsons, R.; VanderNoot, T. *J. Electroanal. Chem.* **1988**, *257*, 9.
(216) Croissant, M. J.; Napporn, T.; Leger, J.-M.; Lamy, C. *Electrochim. Acta* **1998**, *43*, 2447.
(217) Napporn, W. T.; Laborde, H.; Léger, J.-M.; Lamy, C. *J. Electroanal. Chem.* **1996**, *404*, 153.
(218) Napporn, W. T.; Léger, J.-M.; Lamy, C. *J. Electroanal. Chem.* **1996**, *408*, 141.
(219) Maksimov, Y. M.; Gladysheva, T. D.; Podlovchenko, B. I. *Russ. J. Electrochem.* **2001**, *37*, 653.
(220) Venancio, E. C.; Napporn, W. T.; Motheo, A. J. *Electrochim. Acta* **2002**, *47*, 1495.
(221) Mascaro, L. H.; Goncalves, D.; Bulhoes, L. Q. S. *Thin Solid Films* **2004**, *461*, 243.
(222) Lai, E. K. W.; Beattie, P. D.; Holdcroft, S. *Synth. Met.* **1997**, *84*, 87.
(223) Grzeszczuk, M. *Electrochim. Acta* **1994**, *39*, 1809.
(224) Grzeszczuk, M.; Poks, P. *Electrochim. Acta* **2000**, *45*, 4171.
(225) Mikhaylova, A. A.; Molodkina, E. B.; Khazova, O. A.; Bagotzky, V. S. *J. Electroanal. Chem.* **2001**, *509*, 119.
(226) Hable, C. T.; Wrighton, M. S. *Langmuir* **1993**, *9*, 3284.
(227) Lima, A.; Coutanceau, C.; leger, J.-M.; Lamy, C. *J. Appl. Electrochem.* **2001**, *31*, 379.
(228) Lima, A.; Hahn, F.; Leger, J.-M. *Russ. J. Electrochem.* **2004**, *40*, 326.
(229) Grgur, B. N.; Zhuang, G.; Markovic, N. M.; Ross, N. J. *J. Phys. Chem. B* **1997**, *100*, 19538.
(230) Zhang, H.; Wang, Y.; Fachini, E. R.; Cabrera, C. R. *Electrochem. Solid-State Lett.* **1999**, *2*, 437.
(231) Massong, H.; Wang, H.; Samjeske, G.; Baltruschat, H. *Electrochim. Acta* **2000**, *46*, 701.
(232) Jusys, Z.; Xchimdt, T. J.; Duban, L.; Lasch, K.; Jorissen, L.; Garche, J.; Behm, R. J. *J. Power Sources* **2002**, *105*, 297.
(233) Lu, J.; Li, W. S.; Du, J. H.; Fu, Z. M. *J. New Mater. Electrochem. Syst.* **2005**, *8*, 5.
(234) Wu, Y. M.; Li, W. S.; Lu, J.; Du, J. H.; Lu, D. S.; Fu, J. M. *J. Power Soures* **2005**, *145*, 286.
(235) Li, W.; Lu, J.; Du, J.; Lu, D.; Chen, H.; Li, H.; Wu, Y. *Electrochem. Commun.* **2005**, *7*, 406.
(236) Kessler, T.; Castro Luna, A. M. *J. Solid State Electrochem.* **2003**, *7*, 593.
(237) Grace, A. N.; Pandian, K. *Electrochem. Commun.* **2006**, *8*, 1340.
(238) Gupta, V.; Miura, N. *Electrochem. Solid-State Lett.* **2005**, *8*, A630.
(239) Prasad, K. R.; Miura, N. *J. Power Sources* **2004**, *134*, 354.
(240) Zhang, L. X.; Zhang, L. J.; Wan, M. X.; Wei, Y. *Synth. Met.* **2006**, *156*, 454.
(241) Huang, J. X.; Kaner, R. B. *J. Am. Chem. Soc.* **2004**, *126*, 851.
(242) Rajesh, B.; Thampi, K. R.; Bonard, J. M.; Mathieu, H. J.; Xanthopoulos, N.; Viswanathan, B. *Electrochem Solid-State Lett.* **2004**, *7*, A404.
(243) Zhou, H. H.; Jiao, S. Q.; Chen, J. H.; Wei, W. Z.; Kuang, Y. F. *J. Appl. Electrochem.* **2004**, *34*, 455.
(244) Chen, Z.; Xu, L.; Li, W.; Waje, M.; Yan, Y. *Nanotechnology* **2006**, *17*, 5254.
(245) Liu, F.-J.; Huang, L.-M.; Wen, T.-C.; Gopalan, A. *Synth. Met.* **2007**, *157*, 651.
(246) Michel, M.; Ettingshausen, F.; Scheiba, F.; Wolz, A.; Roth, C. *Phys. Chem. Chem. Phys.* **2008**, *10*, 3796.
(247) Niessen, J.; Schroder, U.; Rosenbaum, M.; Scholz, F. *Electrochem. Commun.* **2004**, *6*, 571.
(248) Huang, L.-M.; Tang, W.-R.; Wen, T.-C. *J. Power Sources* **2007**, *164*, 519.
(249) Huang, L.-M.; Chen, C.-H.; Wen, T.-C.; Gopalan, A. *Electrochim. Acta* **2006**, *51*, 2756.
(250) Liu, F.-J.; Huang, L.-M.; Wen, T.-C.; Li, C.-F.; Huang, S.-L.; Gopalan, A. *Synth. Met.* **2008**, *158*, 603.
(251) Hu, Z. A.; Ren, L. J.; Feng, X. J.; Wang, Y. P.; Yang, Y. Y.; Shi, J.; Mo, L. P.; Lei, Z. Q. *Electrochem. Commun.* **2007**, *9*, 97.
(252) Cai, L. T.; Chen, H. Y. *J. Appl. Electrochem.* **1998**, *28*, 161.
(253) Lai, E. K. W.; Beattie, P. D.; Orfino, F. P.; Simon, E.; Holdcroft, S. *Electrochim. Acta* **1999**, *44*, 2559.
(254) Yang, Q.; Wang, Y.; Nakano, H.; Kuwabata, S. *Polym. Adv. Technol.* **2005**, *16*, 759.
(255) Qi, Z.; Lefebvre, M. C.; Pickup, P. G. *J. Electroanal. Chem.* **1998**, *459*, 9.
(256) Warren, M. Electronic and structural effects on the electrochemistry of polypyrrole. B.Sc., The University of British Columbia, 2005.
(257) Chiu, H.-T.; Wu, J.-H. *J. Appl. Polym. Sci.* **2005**, *97*, 711.
(258) Angeli, A. *Gazz. Chim. Ital.* **1916**, *46*, 279.
(259) Diaz, A. F.; Castillo, J. I.; Logan, J. A.; Lee, W.-Y. *J. Electroanal. Chem.* **1981**, *129*, 115 and references therein.
(260) Becerik, İ.; Kadirgan, F. *J. Electroanal. Chem.* **1997**, *436*, 189.
(261) Becerik, İ.; Süzer, S.; Kadirgan, F. *J. Electroanal. Chem.* **1999**, *476*, 171.
(262) Yang; Lu, T.; Xue, K.; Sun, S.; Lu, G.; Chen, S. *J. Electrochem. Soc.* **1997**, *144*, 2302.
(263) Beck, F.; Braun, P.; Oberst, M. *Ber. Bunsen-Ges. Phys. Chem.* **1987**, *91*, 967.
(264) Xue, K. H.; Cai, C. X.; Yang, H.; Zhou, Y. M.; Sun, S. G.; Chen, S. P.; Xu, G. *J. Power Sources* **1998**, *75*, 207.
(265) Becerik, İ.; Kadirgan, F. *Turk. J. Chem.* **2001**, *25*, 373.
(266) Bouzek, K.; Mangold, K.-M.; Jüttner, K. *J. Appl. Electrochem.* **2001**, *31*, 501.
(267) Chandler, G. K.; Pletcher, D. *J. Appl. Electrochem.* **1986**, *16*, 62.
(268) Lee, J. Y.; Tan, T.-C. *J. Electrochem. Soc.* **1990**, *137*, 1402.
(269) Hammache, H.; Makhloufi, L.; Saidani, B. *Synth. Met.* **2001**, *123*, 515.
(270) Sigaud, M.; Li, M.; Chardon-Noblat, S.; José Cadete Santos Aires, F.; Soldo-Olivier, Y.; Simon, J.-P.; Renouprez, A.; Deronzier, A. *J. Mater. Chem.* **2004**, *14*, 2606.
(271) Trueba, M.; Trasatti, S. P.; Trasatti, S. *Mater. Chem. Phys.* **2006**, *98*, 165.
(272) Li, J.; Lin, X. *J. Electrochem. Soc.* **2007**, *154*, B1074.
(273) Ren, X.; Pickup, P. G. *J. Phys. Chem.* **1993**, *97*, 5356.
(274) Lee, H.; Kim, J.; Park, J.; Joe, Y.; Lee, T. *J. Power Sources* **2004**, *131*, 188.
(275) Li, L.; Zhang, Y.; Drillet, J.-F.; Dittmeyer, R.; Jüttner, K.-M. *Chem. Eng. J.* **2007**, *133*, 113.
(276) Feng, C.; Chan, P. C. H.; Hsing, I.-M. *Electrochem. Commun.* **2007**, *9*, 89.
(277) Drillet, J.-F.; Dittmeyer, R.; Jüttner, K.; Li, L.; Mangold, K.-M. *Fuel Cells* **2006**, *6*, 432.
(278) Drillet, J.-F.; Dittmeyer, R.; Jüttner, K. *J. Appl. Electrochem.* **2007**, *37*, 1219.
(279) Kuo, C.-W.; Huang, L.-M.; Wen, T.-C.; Gopalan, A. *J. Power Sources* **2006**, *160*, 65.
(280) Ghosh, S.; Inganas, O. *Adv. Mater.* **1999**, *11*, 1214.
(281) Adamczyk, L.; Kulesza, P. J.; Miecznikowski, K.; Palys, B.; Chojak, M.; Krawczyk, D. *J. Electrochem. Soc.* **2005**, *152*, E98.
(282) Wang, Y. *J. Phys.: Conf. Ser.* **2009**, *152*, 012023.
(283) Kiebooms, R.; Aleshin, A.; Hutchison, K.; Wudl, F. *J. Phys. Chem. B* **1997**, *101*, 11037.
(284) Arbizzani, C.; Biso, M.; Manferrari, E.; Mastragostino, M. *J. Power Sources* **2008**, *180*, 41.
(285) Lefebvre, M. C.; Qi, Z.; Pickup, P. G. *J. Electrochem. Soc.* **1999**, *146*, 2054.
(286) Kelaidopoulou, A.; Abelidou, E.; Kokkinidis, G. *J. Appl. Electrochem.* **1999**, *29*, 1255.
(287) Celebi, M. S.; Pekmez, K.; Özyörük, H.; Yildiz, A. *J. Power Sources* **2008**, *183*, 8.
(288) Choi, J.-H.; Park, K.-W.; Lee, H.-K.; Kim, Y.-M.; Lee, J.-S.; Sung, Y.-E. *Electrochim. Acta* **2003**, *48*, 2781.
(289) Andersson, S.; Collen, B.; Kuylenstierna, U.; Magneli, A. *Acta Chem. Scand.* **1957**, *11*, 1641.
(290) Bartholomew, R.; Frankl, D. *Phys. Rev.* **1969**, *187*, 828.

(291) Marezio, M.; Whan, D. Mc.; Dernier, P.; Remeica, J. *J. Solid State Chem.* **1973**, *6*, 213.
(292) Farndon, E. E.; Pletcher, D. *Electrochim. Acta* **1997**, *42*, 1281.
(293) Przyluski, J.; Kolbrecka, K. *J. Appl. Electrochem.* **1993**, *23*, 1063.
(294) Kolbrecka, K.; Przylski, J. *Electrochim. Acta* **1994**, *39*, 1591.
(295) Smith, J. R.; Walsh, F. C. *J. Appl. Electrochem.* **1998**, *28*, 1021.
(296) Chen, G.; Bare, S. R.; Mallouk, T. E. *J. Electrochem. Soc.* **2003**, *149*, A1092.
(297) Ioroi, T.; Siroma, Z.; Fujiwara, N.; Yamazaki, S.; Yasuda, K. *Electrochem. Commun.* **2005**, *7*, 183.
(298) Ioroi, T.; Senoh, H.; Yamazaki, S.; Siroma, Z.; Fujiwara, N.; Yasuda, K. *J. Electrochem. Soc.* **2008**, *155*, B321.
(299) Dieckmann, G. R.; Langer, S. H. *Electrochim. Acta* **1998**, *44*, 437.
(300) Pollock, R. J.; Houlihan, J. F.; Bain, A. N.; Coryea, B. S. *Mater. Res. Bull.* **1984**, *19*, 17.
(301) Graves, J. E.; Pletcher, D.; Clarke, R. L.; Walsh, F. C. *J. Appl. Electrochem.* **1991**, *21*, 848.
(302) Miller-Folk, R. R.; Noftle, R. E.; Pletcher, D. *J. Electroanal. Chem.* **1989**, *274*, 257.
(303) Park, S.-Y.; Mho, S.-I.; Chi, E. O.; Kwon, Y. U.; Park, H. L. *Thin Solid Films* **1995**, *258*, 5.
(304) He, L.; Franzen, H. F.; Johnson, D. C. *J. Appl. Electrochem.* **1996**, *26*, 785.
(305) Farndon, E. E.; Pletcher, D.; Saraby-Reintjes, A. *Electrochim. Acta* **1997**, *42*, 1269.
(306) Vracar, L. M.; Krstajic, N. V.; Radmilovic, V. R.; Jaksic, M. M. *J. Electroanal. Chem.* **2006**, *587*, 99.
(307) Slavcheva, E.; Nikolova, V.; Petkova, T.; Lefterova, E.; Dragieva, I.; Vitanov, T.; Budevski, E. *Electrochim. Acta* **2005**, *50*, 5444.
(308) Huang, S.-Y.; Ganesan, P.; Park, S.; Popov, B. N. *J. Am. Chem. Soc.* **2009**, *131*, 13898.
(309) Shiih, C.-C.; Chang, J.-R. *J. Catal.* **2006**, *240*, 137.
(310) Sanchez, E.; Lopez, T.; Gomez, R.; Bokhimi, X.; Morales, A.; Novaro, O. *J. Solid State Chem.* **1996**, *122*, 309.
(311) Janssen, M. M. P.; Moolhuysem, J. *Electrochim. Acta* **1976**, *21*, 861.
(312) Andrew, M. R.; McNicoi, B. D.; Short, R. T.; Drury, J. S. *J. Appl. Electrochem.* **1977**, *7*, 158.
(313) Janssen, M. M. P.; Moolhuysen, J. *Electrochim. Acta* **1976**, *21*, 869.
(314) Sekizawa, K.; Widjaja, H.; Maeda, S.; Ozawa, Y.; Eguchi, K. *Catal. Today* **2000**, *59*, 69.
(315) Schryer, D. R.; Upchurch, B. T.; Van Norman, J. D.; Brown, K. G.; Schryer, J. *J. Catal.* **1990**, *122*, 193.
(316) Gardner, S. D.; Hoflund, G. B.; Schryer, D. R.; Upchurch, B. T. *J. Phys. Chem.* **1991**, *95*, 835.
(317) Gadgil, M. M.; Sasikala, R.; Kulshreshtha, S. K. *J. Mol. Catal.* **1994**, *87*, 297.
(318) Okanishi, T.; Matsui, T.; Takeguchi, T.; Kikuchi, R.; Eguchi, K. *Appl. Catal., A* **2006**, *298*, 181.
(319) Baker, W. S.; Pietron, J. J.; Teliska, M. E.; Bouwman, P. J.; Ramaker, D. E.; Swider-Lyons, K. E. *J. Electrochem. Soc.* **2006**, *153*, A1702.
(320) Par, K.-W.; Seol, K.-S. *Electrochem. Commun.* **2007**, *9*, 2256.
(321) Rudorff, W.; Luginsland, H.-H. *Z. Anorg. Allg. Chem.* **1964**, *334*, 125.
(322) Haas, O. E.; Briskeby, S. T.; Kongstein, O. E.; Tsypkin, M.; Tunold, R.; Børresen, B. T. *J. New Mater. Electrochem. Syst.* **2008**, *11*, 9.
(323) García, B. L.; Fuentes, R.; Weidner, J. W. *Electrochem. Solid-State Lett.* **2007**, *10*, B108.
(324) Wang, A.; Xu, H.; Lu, Y.; Hu, J.; Kong, X.; Tian, B.; Dong, H. *Chin. J. Catal.* **2008**, *30*, 179.
(325) Lee, K.-S.; Park, I.-S.; Cho, Y.-H.; Jung, D.-S.; Jung, N.; Park, H.-Y.; Sung, Y.-E. *J. Catal.* **2008**, *258*, 143.
(326) Saraidarov, T.; Reisfeld, R.; Zigansky, E.; Sashchiuk, A.; Lifshitz, E. *Opt. Appl.* **2008**, *38*, 109.
(327) Santos, A. L.; Profeti, D.; Olivi, P. *Electrochim. Acta* **2005**, *50*, 2615.
(328) Pang, H. L.; Zhang, X. H.; Zhong, X. X.; Liu, B.; Wei, X. G.; Kuang, Y. F.; Chen, J. H. *J. Colloid Interface Sci.* **2008**, *319*, 193.
(329) Adachi, M.; Lockwood, D. J. *Self-Organized Nanoscale Materials*; Springer Science+Business Media, Inc.: New York, 2006; p 101.
(330) Bae, C.; Yoo, H.; Kim, S.; Lee, K.; Kim, J.; Sung, M. M.; Shin, H. *Chem. Mater.* **2008**, *20*, 756.
(331) Liang, H.-W.; Liu, S.; Yu, S.-H. *Adv. Mater.* **2010**, *22*, 3925.
(332) Kang, S. H.; Choi, S.-H.; Kang, M.-S.; Hyeon, T.; Sung, Y.-E. *Adv. Mater.* **2008**, *20*, 54.
(333) Bavykin, D. V.; Friedrich, J. M.; Walsh, F. C. *Adv. Mater.* **2006**, *18*, 2807.
(334) Wang, M.; Guo, D.; Li, H. *J. Solid State Chem.* **2005**, *178*, 1996.
(335) Macak, J. M.; Barczuk, P. J.; Tsuchiya, H.; Nowakowska, M. Z.; Ghicov, A.; Chojak, M.; Bauer, S.; Virtanen, S.; Kulesza, P. J.; Schmuki, P. *Electrochem. Commun.* **2005**, *7*, 1417.
(336) Kang, S. H.; Jeon, T.-Y.; Kim, H.-S.; Sung, Y.-E.; Smyrl, W. H. *J. Electrochem. Soc.* **2008**, *155*, B1058.
(337) Kang, S. H.; Sung, Y.-E.; Smyrl, W. H. *J. Electrochem. Soc.* **2008**, *155*, B1128.
(338) Saha, M. S.; Li, R.; Cai, M.; Sun, X. *Electrochem. Solid State Lett.* **2007**, *10*, B130.
(339) Saha, M. S.; Li, R.; Sun, X. *Electrochem. Commun.* **2007**, *9*, 2229.
(340) Butler, M. A. *J. Appl. Phys.* **1977**, *48*, 1914.
(341) Chhina, H.; Campbell, S.; Kesler, O. *J. Electrochem. Soc.* **2007**, *154*, B533.
(342) Abbaro, S. A.; Tseung, A. C. C.; Hibbert, D. B. *J. Electrochem. Soc.* **1980**, *127*, 1106.
(343) Tseung, A. C. C.; Wong, L. *J. Appl. Electrochem.* **1972**, *3*, 211.
(344) Cui, X.; Shi, J.; Chen, H.; Zhang, L.; Guo, L.; Gao, J.; Li, J. *J. Phys. Chem. B* **2008**, *112*, 12024.
(345) Tseung, A. C. C.; Chen, K. Z. *Catal. Today* **1997**, *38*, 439.
(346) Maillard, F.; Peyrelade, E.; Soldo-Olivier, Y.; Chatenet, M.; Chainet, E.; Faure, R. *Electrochim. Acta* **2007**, *52*, 1958.
(347) Kulesza, P. J.; Faulkner, L. R. *J. Electrochem. Soc.* **1989**, *136*, 707.
(348) Micoud, F.; Maillard, F.; Gourgaud, A.; Chatenet, M. *Electrochem. Commun.* **2009**, *11*, 651.
(349) Li, Y. M.; Hibino, M.; Miyayania, M.; Kudo, T. *Solid State Ionics* **2000**, *134*, 271.
(350) Nakajima, H.; Honma, I. *Solid State Ionics* **2002**, *148*, 607.
(351) Park, K. W.; Choi, J. H.; Ahn, K. S.; Sung, Y. E. *J. Phys. Chem. B* **2004**, *108*, 5989.
(352) Jayaraman, S.; Jaramillo, T. F.; Baeck, S. H.; McFarland, E. W. *J. Phys. Chem. B* **2005**, *109*, 22958.
(353) Ganesan, R.; Lee, J. S. *J. Power Sources* **2006**, *157*, 217.
(354) Barczuk, P. J.; Tsuchiya, H.; Macak, J. M.; Schmuki, P.; Szymanska, D.; Makowski, O.; Miecznikowski, K.; Kulesza, P. *Electrochem Solid-State Lett.* **2006**, *9*, E13.
(355) McLeod, E. J.; Birss, V. I. *Electrochim. Acta* **2005**, *51*, 684.
(356) Chen, K. Y.; Tseung, A. C. C. *J. Electrochem. Soc.* **1996**, *143*, 2703.
(357) Raghuveer, V.; Viswanathan, B. *J. Power Sources* **2005**, *144*, 1.
(358) Rajeswari, J.; Viswanathan, B.; Varadarajan, T. K. *Mater. Chem. Phys.* **2007**, *106*, 168.
(359) Maiyalagan, T.; Viswanathan, B. *J. Power Sources* **2008**, *175*, 789.
(360) Ishikawa, A.; Komai, S.; Satsuma, A.; Hattori, T.; Murakami, Y. *Appl. Catal., A* **1994**, *110*, 61.
(361) Hino, M. S.; Kobayashi, S.; Arata, K. *J. Am. Chem. Soc.* **1979**, *101*, 6439.
(362) Hara, S.; Miyayama, M. *Solid State Ionics* **2004**, *168*, 111.
(363) Waqif, M.; Bachelier, J.; Saur, O.; Lavalley, J.-C. *J. Mol. Catal.* **1992**, *72*, 127.
(364) Suzuki, Y.; Ishihara, A.; Mitsushima, S.; Kamiya, N.; Ota, K. *Electrochem. Solid-State Lett.* **2007**, *10*, B105.
(365) Zhang, Y.; Zhang, H.; Zhai, Y.; Zhu, X.; Bi, C. *J. Power Sources* **2007**, *168*, 323.
(366) Skrabalak, S. E.; Suslick, K. S. *J. Am. Chem. Soc.* **2006**, *128*, 12642.

(367) Bang, J. H.; Han, K.; Skrabalak, S. E.; Kim, H.; Suslick, K. S. *J. Phys. Chem. C* **2007**, *111*, 10959.
(368) Messing, G. L.; Zhang, S.-C.; Jayanthi, G. V. *J. Am. Ceram. Soc.* **1993**, *76*, 2707.
(369) Zhu, X.; Zhang, H.; Liang, Y.; Zhang, Y.; Yia, B. *Electrochem Solid-State Lett.* **2006**, *9*, A49.
(370) Watanabe, M.; Motoo, S. *J. Electroanal. Chem.* **1975**, *60*, 267.
(371) Gasteiger, H. A.; Markovic, N.; Ross, P. N.; Cairns, E. *J. Electrochim. Acta* **1994**, *39*, 1825.
(372) Chen, Z.; Qiu, Z.; Lu, B.; Zhang, S.; Zhu, W.; Chen, L. *Electrochem. Commun.* **2005**, *7*, 593.
(373) Wang, L.; Xing, D. M.; Liu, Y. H.; Cai, Y. H.; Shao, Z.-G.; Zhai, Y. F.; Zhong, H. X.; Yi, B. L.; Zhang., H. M. *J. Power Sources* **2006**, *161*, 61.
(374) Seger, B.; Kongkanand, A.; Vinodgopal, K.; Kamat, P. V. *J. Electroanal. Chem.* **2008**, *621*, 198.
(375) Agnihotri, O. P.; Sharma, A. K.; Gupta, B. K.; Thangaraj, R. *J. Phys. D: Appl. Phys.* **1978**, *11*, 643.
(376) Yu, H. Y.; Feng, X. D.; Grozea, D.; Lu, Z. H.; Sodhi, R. N. S.; Hor, A.-M.; Aziz, H. *Appl. Phys. Lett.* **2001**, *78*, 2595.
(377) Chhina, H.; Campbell, S.; Kesler, O. *J. Power Sources* **2006**, *161*, 893.